

研究成果の刊行に関する一覧表

書籍

著者氏名	論文タイトル名	書籍全体の 編集者名	書籍 名	出版社名	出版地	出版年	ページ
なし							

雑誌

発表者氏名	論文タイトル名	発表誌名	巻号	ページ	出版年
Chiaki Katagiri, Kouhei Masuda, Takeshi Urano, Katsumi Yamashita, Yoshio Araki, Kunimi Kikuchi, Hiroshi Shima	Phosphorylation of Ser-446 determines stability of MKP-7	Journal of Biological Chemistry	280巻 15号	14716- 14722	2005年
Sanae Uchida, Akitugu Kubo, Ryoichi Kuzu, Hitoshi Nakagama, Tsukasa Matsunaga, Yukihito Ishizaka, Katsumi Yamashita	Amino acids C- terminal to the 14- 3-3 binding motif in CDC25B affect the efficiency of 14-3- 3 binding	Journal of Biochemistry	印刷中		

研究成果の刊行に関する一覧表レイアウト（参考）

書籍

著者氏名	論文タイトル名	書籍全体の 編集者名	書籍 名	出版社名	出版地	出版年	ページ

雑誌

発表者氏名	論文タイトル名	発表誌名	巻号	ページ	出版年
Nakatsu M, Doshi M, Saeki K, Yuo A	Synergistic effects of dehydroepiandrosteron e and retinoic acid on granulocytic differentiation of human promyelocytic NB4 cells.	Int J Hematol	81	32-38	2005
Saeki K, Yasugi E, Okuma E, Breit SN, Nakamura M, Toda T, Kaburagi Y, Yuo A	Proteomic analysis on insulin signaling in human hematopoietic cells: identification of CLIC1 and SRp20 as novel downstream effectors of insulin.	Am J Physiol Endocrinol Metab	289	E419-E428	2005



Improved gene expression in resting macrophages using an oligopeptide derived from Vpr of human immunodeficiency virus type-1

Izuru Mizoguchi^{a,c}, Yoshihiro Ooe^b, Shigeki Hoshino^a, Mari Shimura^a, Tadashi Kasahara^b, Shigeyuki Kano^{a,c}, Toshiko Ohta^c, Fumimaro Takaku^d, Yasuhide Nakayama^c, Yukihito Ishizaka^{a,*}

^a Research Institute, International Medical Center of Japan, 1-21-1 Toyama, Shinjuku-ku, Tokyo 162-8655, Japan

^b Biochemistry Department, Kyoritsu University of Pharmacy, 1-5-30 Shibakoen, Minato-ku 105-8512, Japan

^c Institute of Basic Medical Sciences, University of Tsukuba, 1-1-1 Ten-nodai, Tsukuba 305-8577, Japan

^d Jichi Medical School, 3311-1 Yakushiji, Minamikawachi-machi, Kawachi-gun, Tochigi 329-0498, Japan

* Department of Bioengineering, Advanced Medical Engineering Center, National Cardiovascular Center Research Institute, 5-7-1 Fujishiro-dai, Suita, Osaka 565-8565, Japan

Received 13 October 2005

Available online 27 October 2005

Abstract

Vpr, an accessory gene product of human immunodeficiency virus type-1, is thought to transport a viral DNA from the cytoplasm to the nucleus in resting macrophages. Previously, we reported that a peptide encompassing amino acids 52–78 of Vpr (C45D18) promotes the nuclear trafficking of recombinant proteins that are conjugated with C45D18. Here, we present evidence that C45D18, when conjugated with a six-branched cationic polymer of poly(*N,N*-dimethylaminopropylacrylamide)-*block*-oligo(4-aminostyrene) (SV: star vector), facilitates gene expression in resting macrophages. Although there was no difference between SV alone and C45D18-SV with respect to gene transduction into growing cells, C45D18-SV resulted in more than 40-fold greater expression of the exogenous gene upon transduction into chemically differentiated macrophages and human quiescent monocyte-derived macrophages. The data suggest that C45D18 contributes to improving the ability of a non-viral vector to transduce macrophages with exogenous genes and we discuss its further application.

© 2005 Elsevier Inc. All rights reserved.

Keywords: HIV-1; Vpr; Nuclear trafficking; Star vector; Gene expression; Resting macrophages

Viral gene transfer systems are commonly used in current gene therapy protocols [1–3], but viral vectors can unfortunately cause side effects, such as severe immunological reactions [4] or leukemogenesis [5]. Thus, it is necessary to develop a non-viral vector system that is both safe and reliable. Various chemical compounds have been synthesized as non-viral vector candidates [6–9], but, in general, they need improvement to allow the expression of the exogenous genes in resting cells [9,10]. Among the obstacles to efficient gene transduction into resting cells is the nuclear

membrane, which constitutes a critical barrier that impairs the efficient expression of exogenous genes [9,11]. Although there have been attempts to circumvent this problem, no reliable method has yet been established for effective transduction into resting cells [12–14].

The *vpr* gene, an auxiliary gene of human immunodeficiency virus type 1 (HIV) [15,16], encodes a virion-associated protein [17–19] and is a crucial factor in HIV-1 infection of resting macrophages [20]. It has been proposed that Vpr transports a pre-integration complex containing the viral DNA from the cytoplasm to the nucleus in infected cells [20]. Vpr has three α -helices (amino acids 17–33, 38–50, and 56–77) [21] but no classical nuclear localization signals [22,23]. It is thought that the nuclear trafficking activity of

* Corresponding author.

E-mail address: zakay@ri.imej.go.jp (Y. Ishizaka).

Vpr is localized in the first and third α -helices [24]. Interestingly, it has been postulated that Vpr transduces proteins as well as plasmid DNA into cells [25,26]. The activity is energy-independent and requires no cellular receptors [27]. A Vpr-derived peptide consisting of amino acids 52–96 has two biological properties that facilitate efficient gene expression: the arginine-rich stretch present in the carboxy (C)-terminal region, at amino acids 80–96, is required for the interaction with plasmid DNA and the third α -helix, at amino acids 52–70, enables trafficking of plasmid DNA through endosomes to the cytoplasm [28].

Recently, we identified a sequence corresponding to amino acids 52–78 (C45D18) as having protein transduction activity (Fig. 1A) [29]. When recombinant proteins are conjugated with C45D18 and added to the culture medium, they are quickly transported to the nucleus. This nuclear trafficking activity of C45D18 is also effective in resting cells, and C45D18-conjugated proteins were incorporated into most cells that were serum-starved during culture, as well as into peripheral blood mononuclear cells. This led us to hypothesize that C45D18 can be used to improve non-viral expression systems applicable to resting cells.

In this study, we combined C45D18 with a non-viral vector system, a cationic polymer named star vector (SV), which is a chemically synthesized gene transfer vector. SV is a nano-structured, hyperbranched, cationic star polymer with highly efficient transduction activity [30–33]. We found that C45D18-SV could induce efficient gene expression in both chemically differentiated macrophages and monocyte-derived macrophages (MDMs). We present the results of an analysis of the expression level of an exogenous gene and incorporated plasmid DNA. We also discuss the mechanism of the improved gene transduction using C45D18 and future applications of the peptide.

Materials and methods

Cell culture and chemicals. HeLa and HT1080 cells were cultured in Dulbecco's modified Eagle's medium (Invitrogen, Carlsbad, CA) supplemented with 10% fetal calf serum (FCS) (Sigma, St. Louis, MI). THP-1 cells (Riken Cell Bank, Tsukuba, Japan) were cultured in Iscove's modified Dulbecco's medium (IMDM) (Invitrogen) supplemented with 10% of FCS. To prepare resting cells, HT1080 cells were cultured for 3 days in 0.1% FCS medium. To differentiate THP-1, aliquots of 1×10^5 cells were plated onto each well of a poly-D-lysine-coated 6-well plate (Beckton-Dickinson, Benford, MA) and treated for 2 days with 5×10^{-8} M phorbol myristate acetate (PMA) (Sigma). The expression of Mac-1, a macrophage marker, was checked with a specific antibody (BD Pharmingen, San Diego, CA). To prepare human MDMs, peripheral blood mononuclear cells obtained from healthy humans were cultured for 4–7 days in the presence of 100 ng/ml of macrophage colony-stimulating factor (M-CSF) (R&D Systems, Minneapolis, MN) [34]. The expression of Mac-1, a macrophage marker, became positive after 2 days of culture (data not shown). For the transduction experiments, MDMs were cultured for an additional 4 days without M-CSF, and then the adherent cells were trypsinized and re-plated at a concentration of 2×10^5 cells per well in a 6-well plate.

Synthesis of hexakis(*N,N*-diethylthiocarbamyl)(oligo(4-aminostyrene)-*b*-block-poly(3-(*N,N*-dimethylamino)propylacrylamide))methylbenzene (6-*star*-PDMAPAAm-*b*-OAS) (SV). Hexakis(bromomethyl)benzene and 4-aminostyrene (AS) (Sigma-Aldrich, Milwaukee, WI), sodium *N,N*-

diethylthiocarbamate (Wako Pure Chemical, Osaka, Japan), and 3-(*N,N*-dimethylamino)propylacrylamide (DMAA) (Tokyo Kasei Kogyo, Tokyo, Japan) were purchased. Other chemical reagents were from Wako. A cationic star polymer with six poly((*N,N*-dimethylamino)propylacrylamide) (PDMAPAAm) chains terminated with oligo(4-aminostyrene) (OAS) per molecule (6-*star*-PDMAPAAm-*b*-OAS) was synthesized by iniferter-based photo-living radical polymerization of DMAA and then AS with hexakis(*N,N*-diethylthiocarbamylmethyl)benzene [32,33]. Briefly, hexakis(*N,N*-diethylthiocarbamylmethyl)benzene was synthesized with reaction of hexakis(bromomethyl)benzene and sodium *N,N*-diethylthiocarbamate, and crystallized from a chloroform-*n*-hexane solution. To synthesize 6-*star*-PDMAPAAm, the mixture of hexakis(*N,N*-diethylthiocarbamylmethyl)benzene and DMAA was irradiated for 30 min with a 200 W high pressure mercury lamp (Spot Cure, Ushio, Tokyo, Japan), concentrated, and dissolved in a small amount of methanol. The precipitate, obtained by the addition to ether (500 ml), was separated by filtration. Reprecipitation was performed in a methanol-ether system three times. The last precipitate was dried under vacuum to give 6-*star*-PDMAPAAm. To produce 6-*star*-PDMAPAAm-*b*-OAS, the mixture of 6-*star*-PDMAPAAm and AS was irradiated for 30 min under the above-mentioned conditions. The reaction mixture was concentrated and precipitated in 500 ml ether. Reprecipitation was carried out in a chloroform-ether system three times. The last precipitate was dried under vacuum to give 6-*star*-PDMAPAAm-*b*-OAS. The total molecular weight was about 18,300, which was estimated from GPC and ^1H NMR spectra. About 17.3 molecules of DMAA unit and 1.4 molecules of AS unit were introduced to each terminal of all the six branch chains in the 6-*star*-PDMAPAAm-*b*-OAS.

Peptide synthesis and conjugation with SV. C45D18, other Vpr-derived peptides (shown in Fig. 1A), and Tat-derived peptide composed of GYGRKRRRQRRRGGC (single-letter amino acid code) [29] were synthesized chemically (Wako). Each peptide contains cysteine in C-terminal region and its SH-residue is used for conjugation to SV compound. Approximately 1 mg of SV was suspended in 1 ml of 10 mM phosphate buffer (pH 7.0) and added to 0.1 mM *N*-[ϵ -maleimidocaproyloxy]succinimide ester (Dojindo Lab. Kumamoto, Japan). After 30 min at room temperature, each peptide was added and further incubated for 3 h at room temperature. The free peptides were removed by dialysis against phosphate-buffered saline overnight. The molar ratio of the peptide to SV was usually 3:1.

Cell cycle analysis. Cells were treated for 30 min, 1 or 2 days with 10 μM bromodeoxyuridine (BrdU) (Sigma). After fixation in 70% ice-cold ethanol, the cells were treated with an anti-BrdU antibody (Beckton-Dickinson) and then detected with Cy3-labelled antibody to mouse IgG (Molecular Probes, Eugene, OR).

Transfection and analysis of transduced genes. pLuc/EGFP constructed with pGL3 (Promega, Madison, WI) and pRES2-EGFP (Clontech, Mountain View, CA) was used as a reporter construct. First, we examined complex formation involving the plasmid DNA and the peptides, SV and C45D18-SV. We incubated 250 ng of plasmid DNA with various amounts of peptides or other compounds in 150 μl Opti-MEM (Invitrogen). After 30 min at room temperature, the aliquots were loaded onto an agarose gel to determine the minimum amount of the compound required to completely neutralize the anionic charge of the DNA and then added to cell culture. After 48 h, luciferase assay was carried out (PicaGene, Toyooka, Tokyo, Japan). The protein concentration was measured by using a Bradford system (Bio-Rad, Hercules, CA) and the relative light units (RLUs) were normalized using the protein concentration.

To examine the level of exogenous gene expression, PCR analysis was carried out on reverse transcribed mRNA of the *GFP* gene. After transfection, mRNA was extracted using RNeasy (Invitrogen), and cDNA was synthesized with oligo(dT) (Qiagen, Hilden, Germany), and then amplified using an EX-Taq polymerase (TaKaRa, Shiga, Japan). To amplify the β -actin or *EGFP* genes, we used the respective forward and reverse primers 5'-TGAACCCCAAGGCCAACC3'-3' and 5'-TTGTGCTGGGTGCC AGGGCA-3' for β -actin or 5'-ATGGTGAGCAAGGGCGA GGA-3' and 5'-TTACTTGTACAGCTCGTCC-3' (Hokkaido System Science, Sapporo, Japan) for *EGFP*. The amplified DNA was applied on an agarose gel, and the electrophoresed DNA was stained with *Vistra Green*

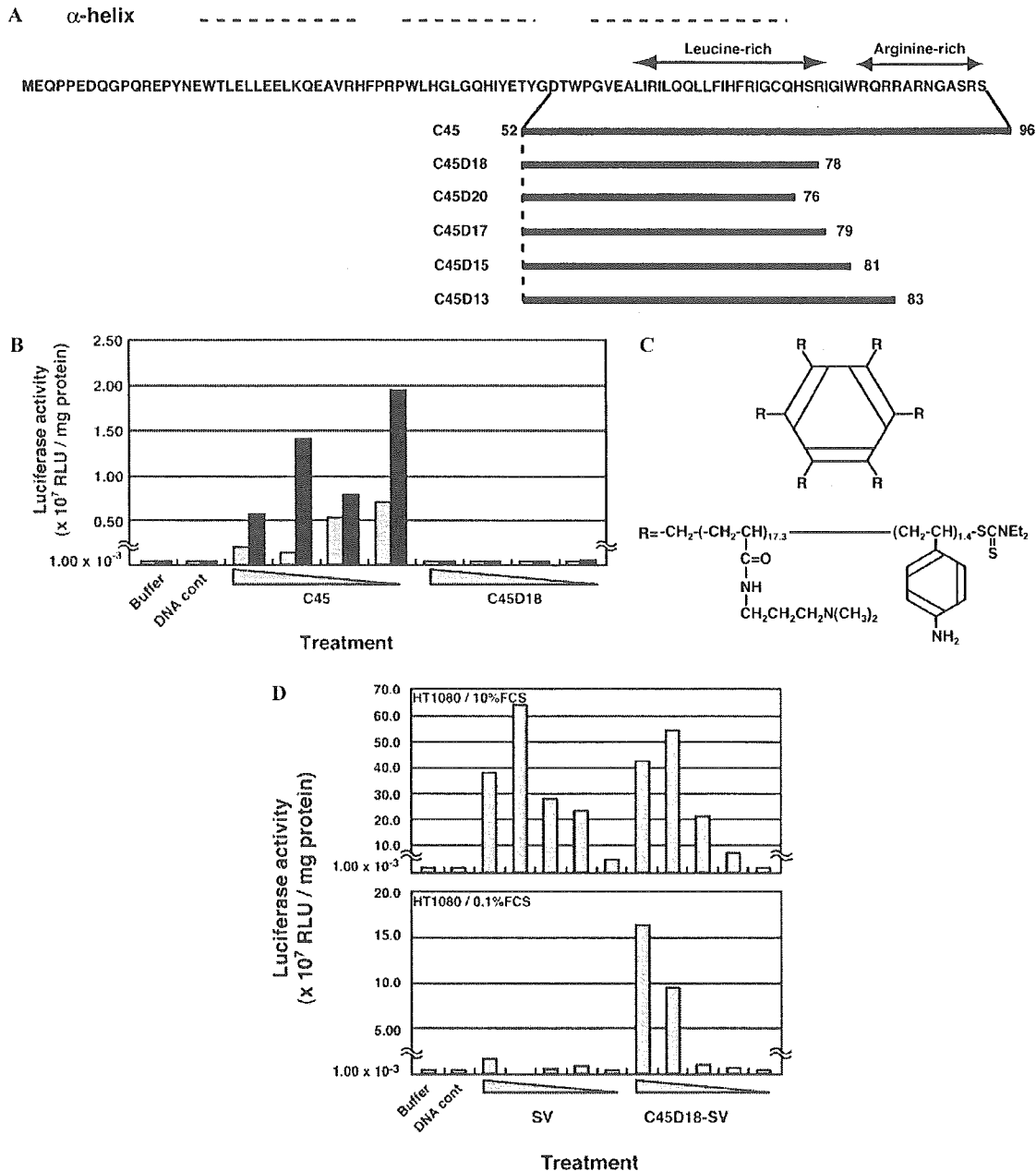


Fig. 1. Gene transduction by C45D18. (A) The amino acid sequences of the peptides used in this study. Amino acids are written using single-letter code. The α -helices and arginine-rich stretch are also shown. Regions corresponding to six Vpr-derived peptides are depicted. (B) Gene transduction by C45 and C45D18 into growing cells. The reporter plasmid DNA, pLuc/EGFP, was mixed with C45 or C45D18, and was then added to HeLa (gray columns) or THP-1 (black columns) cells. Various concentrations of the peptides, ranging from 400 to 15 μM , were used. One representative result out of three independent experiments is shown. Luciferase activity is shown as relative light units (RLUs)/mg protein. (C) Schematic structure of SV. The SV used in this study has six branches (shown by "R") (21). The arrow indicates the amino residue that is used for conjugation with various peptides. (D) Efficient gene transduction by C45D18 into serum-starved cells. The gene transduction efficiencies using C45D18-SV and SV were compared. The HT1080 cells were cultured for 3 days in the presence of 0.1% FCS (lower panel) or under normal conditions (upper panel) and were then used for the experiments. The respective frequencies of BrdU-positive cells in the population were 9% and 43% for serum-starved cells and those cultured in the presence of 10% FCS, respectively. For each sample, 250 ng of plasmid DNA was mixed with 45–1.4 μM of the compounds.

(Amersham Biosciences, Piscataway, NJ). Then, the signal intensity of each band was measured using FX-PRO PLUS (Bio-Rad).

To analyze the plasmid DNAs incorporated in the nuclei, an aliquot of plasmid DNA was labeled with Cy3-dCTP (Amersham Biosciences), mixed with the same amount of plasmid DNA, and then used for trans-

fection. The incorporated plasmid DNA was visualized using laser scanning microscopy (Bio-Rad). Cells positive for DNA aggregates that were larger than 2 μm were counted.

Statistical analysis. Statistical significance was evaluated using Student's *t* test.

Results

Gene transduction with C45 and C45D18

First, we compared the gene transduction activity of two peptides, C45 and C45D18 (Fig. 1A). Based on the results of a gel-shift assay to monitor the lipoplex formation of pLuc/EGFP (250 ng) with C45 (see Materials and methods), we used 15, 45, 135, and 400 μ M of the peptide for the experiment. The C45 and an equivalent amount of C45D18 were incubated with plasmid DNA for 30 min at room temperature and were then added to cultures of HeLa and THP-1 cells. Consistent with previous reports [35,36], C45 was effective for gene transduction into these cells (Fig. 1B). By contrast, C45D18 did not show any transduction activity.

C45D18 facilitates gene transduction into resting cells

We previously reported that recombinant proteins, when conjugated with C45D18, could be transported into the nuclei of resting cells [29]. This finding led us to postulate that C45D18 could facilitate gene expression in resting cells, if an appropriate vehicle for the DNA were selected. To prove this, C45D18 was conjugated to SV (C45D18-SV; Fig. 1C), and we compared the efficiency of gene transduction using C45D18-SV with that using SV alone. Although the gene expression in growing cells was equivalent with both agents (Fig. 1D, upper panel), C45D18-SV resulted in more efficient gene expression in cells that had been cultured in the presence of 0.1% FCS (Fig. 1D, lower panel). Analysis of the cell cycle, judged using incorporated BrdU, revealed that the number of cells in S phase was decreased remarkably in the populations cultured in 0.1% FCS (9%) as compared with those cultured in 10% FCS (43%).

C45D18-SV increased the gene transfer to human macrophages

To obtain stronger evidence that C45D18 facilitates gene transduction into resting cells, we used THP-1 cells that had been treated with PMA. THP-1 is a non-adherent human monocytic leukemia cell line that acquires the macrophage-phenotype when cultured in the presence of PMA. Within 2 days after PMA treatment, THP-1 cells became adherent and positive for Mac-1, a macrophage-specific marker (data not shown). Then, we tested the efficacy of gene transduction using C45D18-SV. As shown in Fig. 2A, luciferase expression with C45D18-SV transduction was more than 40 times that with SV alone ($p < 0.05$). To examine the expression level of the exogenous gene, we amplified the *GFP* mRNA from transfectants treated with SV alone or with C45D18-SV and compared the intensities of the amplified DNA. As shown in Fig. 2B, the level of gene expression was increased strikingly in the cells treated with C45D18-SV (lane 2). Pulse-labeling with BrdU followed by detection with anti-BrdU

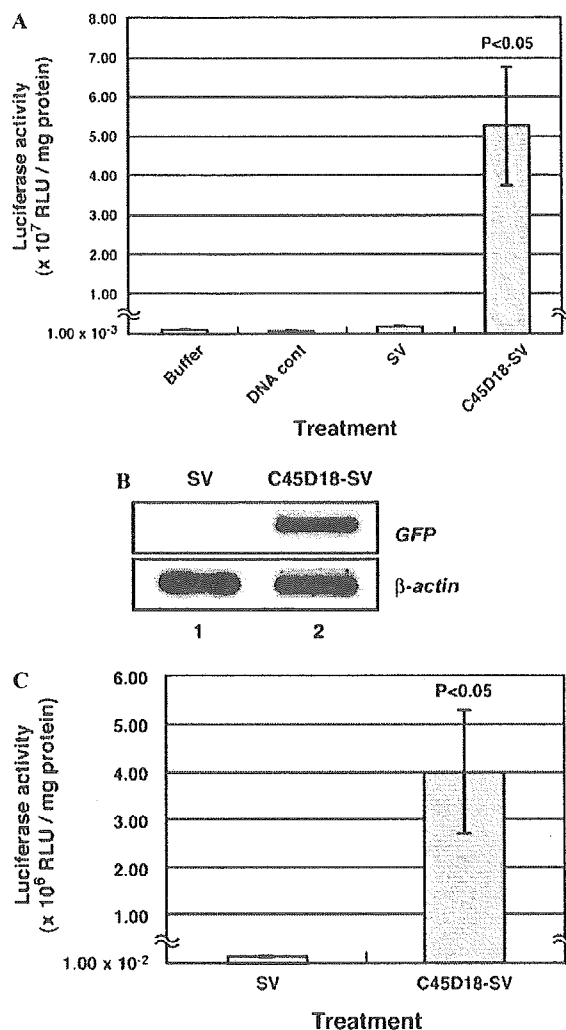


Fig. 2. Increased gene expression using C45D18-SV in resting macrophages. (A) The effects of C45D18-SV on chemically differentiated macrophages. THP-1 cells, after treatment for 2 days with PMA, were used for the transfection experiments. The experiments were carried out in triplicate, and the mean numbers and standard deviation were calculated. BrdU incorporation indicated that less than 1% of the cells were at S phase. Even with continuous exposure to BrdU for 2 days after transfection, less than 1% of the cells were BrdU-positive. (B) The expression of the exogenous gene using C45D18-SV in resting macrophages. RT-PCR analysis was performed using THP-1 cells treated with PMA and then transfected. As an internal control, β -actin mRNA was amplified. The results of the RT-PCR analysis of cells transfected using SV (lane 1) and C45D18-SV (lane 2) are shown. (C) Gene transduction into human macrophages. MDMs were prepared from healthy humans by culturing peripheral blood mononuclear cells for 6 days in the presence of 100 ng/ml M-CSF. Then, the cells were deprived of M-CSF for 4–5 days and subjected to experiments in triplicate. The mean value and standard deviation are shown, along with a representative result of three independent experiments. Immunohistochemical analyses of pulse-labeled BrdU and Mac-1 indicate that the prepared cells were resting macrophages (data not shown).

antibody revealed that less than 1% of PMA-treated THP-1 cells were positive for BrdU incorporation (data not shown), whereas about 30% of the untreated THP-1 cells were positive for BrdU incorporation. Moreover, with

continuous exposure to BrdU for 2 days after transfection, only 0.6% of the PMA-treated cells were labeled with BrdU (data not shown). These results indicate that THP-1 cells stop growing within 2 days after treatment with PMA and that C45D18-SV facilitates gene expression in resting macrophages.

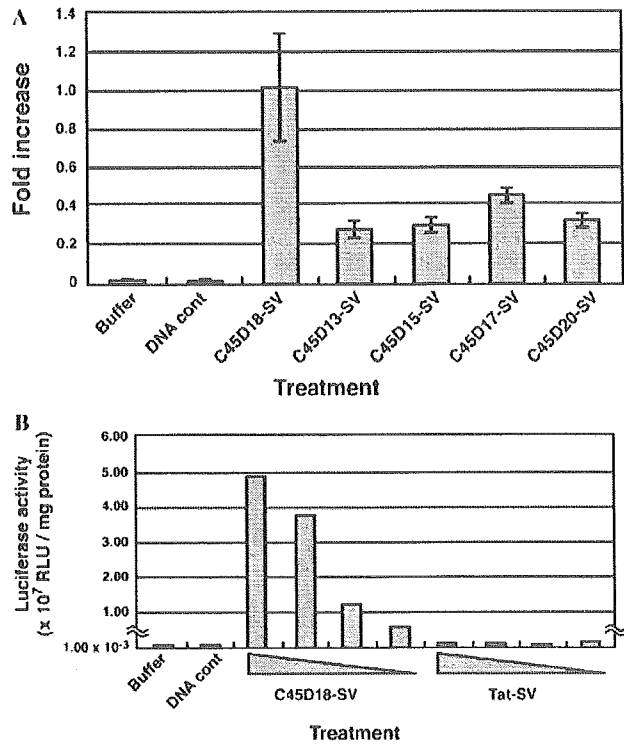
Next, we focused on gene transduction into human MDMs using C45D18-SV. To test the efficacy of C45D18-SV, human macrophages were prepared by culturing peripheral blood mononuclear cells for 6 days in the presence of 100 ng/ml M-CSF. After cell expansion, the M-CSF was removed from the culture, and the culture was continued for another 4–5 days, which caused the expanded MDMs to stop growing (data not shown). Using these cells, we investigated the efficacy of C45D18. As shown in Fig. 2C, the transduction efficiency with C45D18-SV was significantly greater than that with SV alone ($p < 0.05$). We repeated the same experiments three times and obtained essentially the same statistically significant results.

C45D18-SV is the best molecule for gene transduction into macrophages

To determine the best Vpr-derived peptide for gene transfer into macrophages, several peptides were synthesized (Fig. 1A) and conjugated to SV at a molar ratio of 3:1. First, we compared the activities of C45 and C45D18. As shown in Table 1, C45-SV was much less potent than C45D18-SV in resting macrophages ($p < 0.01$), which is in contrast to the result, shown in Fig. 1B, that C45 induced much better gene expression in growing cells than did C45D18.

Next, we compared the activity of C45D18 with those of four other peptides. Based on several independent experiments, we estimated that the gene transduction efficiencies with C45D17, C45D15, C45D13, and C45D20 relative to that with C45D18 (1.0) were 0.25, 0.30, 0.45, and 0.32, respectively (Fig. 3A). Therefore, C45D18 is the minimum sequence giving the best efficiency of gene expression in resting macrophages.

Protein transduction activity has been well documented for Tat-derived peptide. Although the gene transduction activity of Tat has not been reported, we compared the



^a The relative right units (RLUs) were normalized using the protein concentration. The mean values and standard deviations were calculated from triplicate samples. Difference between luciferase activity obtained by C45-SV and C45D18-SV was statistically significant ($p < 0.01$).

^b The fold increase was estimated using data for the buffer as control.

Fig. 3. C45D18 is the best molecule for efficient gene expression in resting macrophages. (A) Comparison of the gene transduction activities among C45D18 and four Vpr-derived peptides (see Fig. 1A). Each peptide was conjugated to SV at a molar ratio of 3:1, and the efficiency of gene expression in resting macrophages was analyzed. For each peptide, 17 μ M peptide was reacted with 250 ng pLuc/EGFP. Three independent experiments were performed, and the mean and standard deviation were calculated. The activity of each peptide is given as a relative efficiency by defining the activity of C45D18-SV as 1.0. The actual luciferase activity obtained with C45D18-SV was $5.2 \pm 1.6 \times 10^7$ RLU/mg protein. (B) The effects of Tat-derived peptide on gene transfer into resting macrophages. Tat-derived peptide was conjugated to SV at a molar ratio of 3:1, and then the efficiency of gene expression in resting macrophages was examined. The maximum dose of each conjugated compound was 12 μ M with 250 ng plasmid DNA. Each compound was serially diluted to 6, 3, and 1.5 μ M, and the compound was reacted with the reporter plasmid DNA.

gene transduction efficiency of Tat and C45D18. As shown in Fig. 3B, Tat-conjugated SV did not result in significant expression of the exogenous gene, whereas C45D18-SV reproducibly induced high expression from the plasmid DNA in resting macrophages.

Condensed localization of exogenous DNA in the nucleus using C45D18-SV

To characterize the DNA incorporated in the nucleus by C45D18, we investigated the plasmid DNA in resting macrophages after transfection. For this purpose, an aliquot of plasmid DNA was labeled with Cy3-dCTP, mixed with an equal amount of unlabeled DNA, and used for the transfection experiment. Surprisingly, we observed the presence of plasmid DNA as large dots in the nucleus when C45D18-SV was used as the vector (Fig. 4A, right panels),

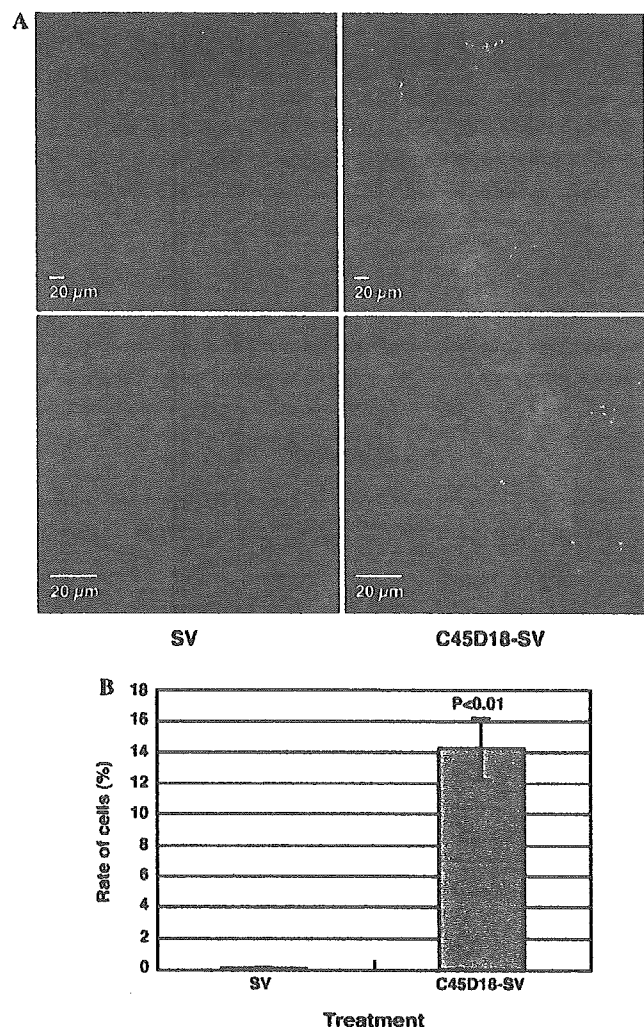


Fig. 4. Analysis of plasmid DNA introduced using C45D18-SV. (A) The aggregation of exogenous DNA in cells transduced with C45D18-SV. Plasmid DNA incorporated with SV (left panels) or C45D18-SV (right panels) was visualized using laser scanning microscopy. A small amount of plasmid DNA that had been pre-labeled with Cy3 was mixed with an equal amount of unlabeled plasmid DNA. The lower panels show enlarged cells. Plasmid DNA and nuclear DNA are shown in red and blue, respectively. The scale bar indicates 20 μm . (B) Increased number of cells with aggregated plasmid DNA. The number of cells containing large dots of plasmid DNA ($>2 \mu\text{m}$) was counted and plotted. At least 100 cells were counted per microscopic field. The mean and standard deviation were calculated using data obtained from three independent experiments. The difference between cells transduced using SV and those transduced using C45D18-SV was statistically significant ($p < 0.01$). (For interpretation of the references to color in this figure legend, the reader is referred to the web version of this paper.)

whereas fine dots of DNA were present in the cells transfected with SV alone (Fig. 4B, left panels). We counted the number of cells that contained labeled plasmid DNA dots larger than 2 μm . As shown in Fig. 4B, C45D18-SV dramatically increased the number of cells containing large dots of plasmid DNA; about 15% of the cells transduced with C45D18-SV contained large dots of aggregated plasmid DNA ($p < 0.01$). PCR analysis indicated that the copy

number of plasmid DNA in cells treated with C45D18-SV was at most 1.7-fold that in cells treated with SV (data not shown).

Discussion

C45D18-SV is an effective, novel non-viral vector for gene transduction into human macrophages

We showed that C45D18 facilitates gene transduction into resting macrophages. In this work, we used SV as a vehicle for the plasmid DNA. SV is a synthetic cationic polymer used as a gene transfer vector [30]. It was previously demonstrated that SV can induce a gene transduction level 10-fold that induced with polyethylenimine (PEI), which is one of the best agents popularly used for gene transfer [30]. Although SV by itself was not effective for introducing genes into chemically differentiated macrophages, C45D18-SV could promote the expression of exogenous genes at a significantly higher level (Figs. 2A and B). Furthermore, C45D18-SV could facilitate the expression of an exogenous gene in quiescent human MDMs (Fig. 2C). These results are consistent with our previous report that recombinant proteins conjugated with C45D18 could be transported into the nuclei of resting cells [29]. Based on these observations, we postulate that the C45D18-SV system will be effective for other types of resting cells. This possibility is now under investigation.

Of the peptides with protein transduction activity, it has been reported that Tat can transduce recombinant proteins, which are expressed as chimeric forms with Tat-derived peptide. In this work, we also tested the activity of the Tat-derived peptide, but Tat-SV induced few exogenous genes in resting macrophages (Fig. 3B). Therefore, C45D18 is the best candidate molecule for circumventing the difficulties of non-viral vector systems applied to resting cells.

Differential activity of C45D18 and C45

Interestingly, we observed a functional difference between C45 and C45D18. As reported [35,36], C45 could express plasmid DNA in growing cells (Fig. 1B), whereas C45D18 could not cause transduction alone; however, after conjugation to a cationic polymer, C45D18 showed unique activity, enabling gene expression in resting macrophages. By contrast, C45-SV was much less effective for gene transduction into resting cells (Table 1).

Vpr binds DNA through its C-terminal region [37]. C45D18 lacks the C-terminal region that is required for DNA binding, which explains why C45D18 alone could not cause gene expression. With C45D18 conjugated to SV, the cationic moiety of SV complemented the DNA binding property, restoring the nuclear trafficking activity of C45D18, which led to the transduction of genes into resting macrophages. By contrast, the conjugation of C45

to SV decreased its ability to cause gene expression in resting cells (Table 1). Both C45D18 and C45 were conjugated to SV through the cysteine residue at amino acid 76 of Vpr (see Materials and methods, and Fig. 1A). One possible explanation as to why C45 activity was decreased after conjugation to SV is that the interaction between the cationic moieties of C45 and SV interferes with the properties of the leucine/isoleucine-rich domain (LR-domain) of Vpr [23] (Fig. 1A). The LR-domain (amino acids 60–81) was reported to be required for nuclear trafficking of Vpr, and point mutations at amino acids 64, 67, 71, and 76 significantly reduced the Vpr activity of nuclear trafficking [24]. It would be important to conjugate C45D18 to other compounds through the third position of its C-terminal region to keep the amino half of C45D18 fully functional. In this context, it is likely that the nuclear trafficking activity of C45D18, if conjugated appropriately, would contribute to non-viral vector systems other than SV.

Effects of C45D18 on transduced plasmid DNA

Strikingly, the incorporated DNA aggregated in the nucleus when C45D18-SV was used as a transfer vector (Fig. 4A). About 15% of the cells were positive for large dots of plasmid DNA ($>2 \mu\text{m}$). By contrast, we detected few such cells after transduction by SV alone. It is still not known whether aggregated molecules are effective for gene expression. Although RT-PCR demonstrated that C45D18-SV strongly induced the expression of an exogenous gene (Fig. 2B), PCR analysis of the transduced DNA revealed that C45D18-SV did not dramatically increase the copy number of the exogenous gene, but gave at most 1.7 times the plasmid DNA produced with SV. These data suggest that C45D18-SV increased the local concentration of the plasmid DNA, resulting in increased expression of the exogenous gene.

The aggregation of plasmid DNA by C45D18 may impair the expression of the exogenous gene. When genes are transduced using a non-viral gene transfer system, the plasmid DNA must be released from the gene-transducing agent for efficient gene expression [38]. If the plasmid DNA transduced into nucleus is surrounded by the gene transfer agent, for example, by PEI, transcription cannot effectively occur [39]. When we examined the numbers of cells with exogenous gene expression, less than 1% of total cells were positive for GFP expression. Even in an immunohistochemical analysis with anti-GFP antibody, we observed that GFP-positive cells, indicating the transducing efficiency of the exogenous gene, increased to 0.5% from 0.1% on using C45D18-SV compared with SV alone. The data indicate that C45D18 increased the number of cells that are positive for expression of exogenous DNA, but most of the plasmid DNA transported into the nucleus unfortunately does not work well as a template for transcription. It is still necessary to develop a system in which exogenous genes transported to the nucleus by C45D18 are effectively released for favorable gene expression.

Acknowledgments

We thank Dr. Koetsu Ogasawara for offering advice regarding this study. This work was supported by a Grant-in-Aid for Scientific Research from the Ministry of Health, Labor and Welfare of Japan.

References

- [1] G. Romano, P.P. Claudio, H.E. Kaiser, A. Giordano, Recent advances, prospects and problems in designing new strategies for oligonucleotide and gene delivery in therapy, *In Vivo* 12 (1998) 59–67.
- [2] G. Romano, P. Michell, C. Pacilio, A. Giordano, Latest developments in gene transfer technology: achievements, perspectives, and controversies over therapeutic applications, *Stem Cells* 18 (2000) 19–39.
- [3] K.K. Hunt, S.A. Vorburger, Tech. Sight. Gene therapy. Hurdles and hopes for cancer treatment, *Science* 297 (2002) 415–416.
- [4] N. Boyce, In memoriam: tougher rules could be the legacy of gene therapy's first death, *New Sci.* 164 (1999) 9.
- [5] J. Kaiser, Gene therapy. Seeking the cause of induced leukemias in X-SCID trial, *Science* 299 (2003) 495.
- [6] H. Ma, S.L. Diamond, Nonviral gene therapy and its delivery systems, *Curr. Pharm. Biotechnol.* 2 (2001) 1–17.
- [7] U. Lungwitz, M. Breunig, T. Blunk, A. Gopferich, Polyethylenimine-based non-viral gene delivery systems, *Eur. J. Pharm. Biopharm.* 60 (2005) 247–266.
- [8] Y. Nagasaki, K. Yasugi, Y. Yamamoto, A. Harada, K. Kataoka, Sugar-installed block copolymer micelles, their preparation and specific interaction with lectin molecules, *Biomacromolecules* 2 (2001) 1067–1070.
- [9] D.A. Dean, D.D. Strong, W.E. Zimmer, Nuclear entry of nonviral vectors, *Gene Ther.* 12 (2005) 881–890.
- [10] A. Fasbender, J. Zabner, B.G. Zeiher, M.J. Welsh, A low rate of cell proliferation and reduced DNA uptake limit cationic lipid-mediated gene transfer to primary cultures of ciliated human airway epithelia, *Gene Ther.* 4 (1997) 1173–1180.
- [11] F.M. Munkonge, D.A. Dean, E. Hillery, U. Griesenbach, E.W. Alton, Emerging significance of plasmid DNA nuclear import in gene therapy, *Adv. Drug. Deliv. Rev.* 55 (2003) 749–760.
- [12] J. Zabner, A.J. Fasbender, T. Moninger, K.A. Poellinger, M.J. Welsh, Cellular and molecular barriers to gene transfer by a cationic lipid, *J. Biol. Chem.* 270 (1995) 18997–19007.
- [13] T.K. Prasad, N.M. Rao, The role of plasmid constructs containing the SV40 DNA nuclear-targeting sequence in cationic lipid-mediated DNA delivery, *Cell. Mol. Biol. Lett.* 10 (2005) 203–215.
- [14] S. Brunner, T. Sauer, S. Carotta, M. Cotten, M. Saltik, E. Wagner, Cell cycle dependence of gene transfer by lipoplex, polyplex and recombinant adenovirus, *Gene Ther.* 7 (2000) 401–407.
- [15] F. Wong-Staal, P.K. Chanda, J. Ghayeb, Human immunodeficiency virus: the eighth gene, *AIDS Res. Hum. Retroviruses* 3 (1987) 33–39.
- [16] E.A. Cohen, R.A. Subbramanian, H.G. Gottlinger, Role of auxiliary proteins in retroviral morphogenesis, *Curr. Top. Microbiol. Immunol.* 214 (1996) 219–235.
- [17] X.F. Yu, M. Matsuda, M. Essex, T.H. Lee, Open reading frame vpr of simian immunodeficiency virus encodes a virion-associated protein, *J. Virol.* 64 (1990) 5688–5693.
- [18] W. Paxton, R.I. Connor, N.R. Landau, Incorporation of vpr into human immunodeficiency virus type 1 virions: requirement for the p6 region of gag and mutational analysis, *J. Virol.* 67 (1993) 7229–7237.
- [19] E.A. Cohen, G. Dehni, J.G. Sodroski, W.A. Haseltine, Human immunodeficiency virus vpr product is a virion-associated regulatory protein, *J. Virol.* 64 (1990) 3097–3099.

- [20] M.A. Vodicka, D.M. Koepf, P.A. Silver, M. Emerman. HIV-1 Vpr interacts with the nuclear transport pathway to promote macrophage infection. *Genes Dev.* 12 (1998) 175–185.
- [21] N. Morellet, S. Bouaziz, P. Petitjean, B.P. Roques, NMR structure of the HIV-1 regulatory protein VPR, *J. Mol. Biol.* 327 (2003) 215–227.
- [22] C. Dingwall, R.A. Laskey, Nuclear targeting sequences—a consensus? *Trends Biochem. Sci.* 16 (1991) 478–481.
- [23] L.J. Zhao, S. Mukherjee, O. Narayan, Biochemical mechanism of HIV-1 Vpr function. Specific interaction with a cellular protein. *J. Biol. Chem.* 269 (1994) 15577–15582.
- [24] S. Mahalingam, V. Ayyavoo, M. Patel, T. Kieber-Emmons, D.B. Weiner, Nuclear import, virion incorporation, and cell cycle arrest/differentiation are mediated by distinct functional domains of human immunodeficiency virus type 1 Vpr, *J. Virol.* 71 (1997) 6339–6347.
- [25] M.P. Sherman, U. Schubert, S.A. Williams, C.M. de Noronha, J.F. Kreisberg, P. Henklein, W.C. Greene, HIV-1 Vpr displays natural protein-transducing properties: implications for viral pathogenesis, *Virology* 302 (2002) 95–105.
- [26] S.C. Piller, G.D. Ewart, A. Premkumar, G.B. Cox, P.W. Gage, Vpr protein of human immunodeficiency virus type 1 forms cation-selective channels in planar lipid bilayers, *Proc. Natl. Acad. Sci. USA* 93 (1996) 111–115.
- [27] P. Henklein, K. Bruns, M.P. Sherman, U. Tessmer, K. Licha, J. Kopp, C.M. de Noronha, W.C. Greene, V. Wray, U. Schubert, Functional and structural characterization of synthetic HIV-1 Vpr that transduces cells, localizes to the nucleus, and induces G2 cell cycle arrest, *J. Biol. Chem.* 275 (2000) 32016–32026.
- [28] Y. Jenkins, M. McEntee, K. Weis, W.C. Greene, Characterization of HIV-1 vpr nuclear import: analysis of signals and pathways, *J. Cell Biol.* 143 (1998) 875–885.
- [29] T. Taguchi, M. Shimura, Y. Osawa, Y. Suzuki, I. Mizoguchi, K. Niino, F. Takaku, Y. Ishizaka, Nuclear trafficking of macromolecules by an oligopeptide derived from Vpr of human immunodeficiency virus type-1, *Biochem. Biophys. Res. Commun.* 320 (2004) 18–26.
- [30] Y. Nakayama, T. Masuda, M. Nagaishi, M. Hayashi, M. Ohira, M. Harada-Shiba, High performance gene delivery polymeric vector: nano-structured cationic star polymers (Star vectors), *Curr. Drug Deliv.* 2 (2005) 53–57.
- [31] Y. Nakayama, T. Matsuda, Surface macromolecular architectural designs using photo-graft copolymerization based on photochemistry of benzyl *N,N*-diethyldithiocarbamate, *Macromolecules* 29 (1996) 8622–8630.
- [32] Y. Nakayama, M. Miyamura, Y. Hirano, K. Goto, T. Matsuda, Preparation of poly (ethylene glycol)-polystyrene block copolymers using photochemistry of dithiocarbamate as a reduced cell-adhesive coating material, *Biomaterials* 20 (1999) 963–970.
- [33] Y. Nakayama, T. Matsuda, Surface macromolecular microarchitecture design: biocompatible surfaces via photo-block-graft-copolymerization using *N,N* diethyldithiocarbamate, *Langmuir* 15 (1999) 5560–5566.
- [34] G. Li, Y.J. Kim, H.E. Broxmeyer, Macrophage colony-stimulating factor drives cord blood monocyte differentiation into IL-10(high)IL-12absent dendritic cells with tolerogenic potential, *J. Immunol.* 174 (2005) 4706–4717.
- [35] A. Kichler, J.C. Pages, C. Leborgne, S. Druillennec, C. Lenoir, D. Coulaud, E. Delain, E. Le Cam, B.P. Roques, O. Danos, Efficient DNA transfection mediated by the C-terminal domain of human immunodeficiency virus type 1 viral protein R, *J. Virol.* 74 (2000) 5424–5431.
- [36] E. Coeytaux, D. Coulaud, E. Le Cam, O. Danos, A. Kichler, The cationic amphipathic alpha-helix of HIV-1 viral protein R (Vpr) binds to nucleic acids, permeabilizes membranes, and efficiently transfects cells, *J. Biol. Chem.* 278 (2003) 18110–18116.
- [37] S. Zhang, D. Pointer, G. Singer, Y. Feng, K. Park, L.J. Zhao, Direct binding to nucleic acids by Vpr of human immunodeficiency virus type 1, *Gene* 212 (1998) 157–166.
- [38] M.B. Bally, P. Harvie, F.M. Wong, S. Kong, E.K. Wasan, D.L. Reimer, Biological barriers to cellular delivery of lipid-based DNA carriers, *Adv. Drug. Deliv. Rev.* 38 (1999) 291–315.
- [39] V.K. Sharma, M. Thomas, A.M. Klibanov, Mechanistic studies on aggregation of polyethylenimine–DNA complexes and its prevention, *Biotechnol. Bioeng.* 90 (2005) 614–620.

HIV-1 Vpr Induces DNA Double-Strand Breaks

Hiroaki Tachiwana,^{1,2} Mari Shimura,² Chikako Nakai-Murakami,²
Kenzo Tokunaga,³ Yoshimasa Takizawa,^{1,2} Tetsutaro Sata,³
Hitoshi Kurumizaka,¹ and Yukihito Ishizaka²

¹Graduate School of Science and Engineering, Waseda University; ²Department of Intractable Diseases, International Medical Center of Japan; and ³Department of Pathology, National Institute of Infectious Diseases, Tokyo, Japan

Abstract

Recent observations imply that HIV-1 infection induces chromosomal DNA damage responses. However, the precise molecular mechanism and biological relevance are not fully understood. Here, we report that HIV-1 infection causes double-strand breaks in chromosomal DNA. We further found that Vpr, an accessory gene product of HIV-1, is a major factor responsible for HIV-1-induced double-strand breaks. The purified Vpr protein promotes double-strand breaks when incubated with isolated nuclei, although it does not exhibit endonuclease activity *in vitro*. A carboxyl-terminally truncated Vpr mutant that is defective in DNA-binding activity is less capable of Vpr-dependent double-strand break formation in isolated nuclei. The data suggest that double-strand breaks induced by Vpr depend on its DNA-binding activity and that Vpr may recruit unknown nuclear factor(s) with positive endonuclease activity to chromosomal DNA. This is the first direct evidence that Vpr induces double-strand breaks in HIV-1-infected cells. We discuss the possible roles of Vpr-induced DNA damage in HIV-1 infection and the involvement of Vpr in further acquired immunodeficiency syndrome-related tumor development. (Cancer Res 2006; 66(2): 627-31)

Introduction

A high incidence of malignant tumors, such as non-Hodgkin's lymphoma, Kaposi's sarcoma, and invasive cervical cancer [acquired immunodeficiency syndrome (AIDS)-defining cancers], is epidemiologically associated with HIV-1 infection (1, 2). These neoplasms are attributable mainly to diseases that accompany immunodeficiency, including coinfection with EBV, human herpes virus 8, and human papillomavirus (1, 2). In addition to these AIDS-defining cancers, several non-AIDS-defining cancers also occur with a higher incidence in HIV-infected individuals (3, 4). These reports lead to the assumption that HIV-1 has the potential to induce neoplasms before AIDS develops. Recently, DNA damage responses have been observed in precancerous lesion before inactivation of p53 (5, 6). Interestingly, it has been reported that HIV-1 infection induces DNA damage responses by activating Rad3-related or ataxia-telangiectasia mutated proteins and pro-

moting phosphorylation of their downstream substrates (7, 8). The elucidation of the factor triggering the DNA damage responses to HIV-1 infection is essential to determine the as yet unknown mechanism causing AIDS-related neoplasms. In the present study, we found that HIV-1 infection induces double-strand breaks of chromosomal DNA, as detected using pulsed-field gel electrophoresis (PFGE). We further showed that *vpr*, an accessory gene of HIV-1 encoding a virion-associated nuclear protein, which induces cell cycle accumulation at G₂-M phase and increases ploidy (9), was a factor responsible for double-strand breaks. We discuss the potential ability of Vpr-induced double-strand breaks to develop into neoplasms in HIV-1 infection.

Materials and Methods

Cell culture. MIT-23 and ΔVpr, a mock transfectant, were established from HT1080 (JCRB9113; the Health Science Research Resources Bank) as previously described (9). In MIT-23, Vpr expression is controlled by the *ret* promoter on incubation with 3 μg/mL doxycycline (Sigma, St. Louis, MO) for 48 hours.

Virus infection. Vesicular stomatitis virus G protein (VSV-G)-pseudotyped HIV-1 was produced by cotransfection with a plasmid encoding VSV-G (pHIT/G) and the pNL-Luc-E R⁺ or pNL-Luc-E R⁻ proviral clone (10). The preparation and titration of viruses are described elsewhere (11). Briefly, the concentration of p24 antigen in the culture supernatant was measured using a p24 Gag antigen capture ELISA kit (ZeptoMetrix, Buffalo, NY). The infectivity of the prepared viral stock was examined using MAGIC5 cells. HT1080 cells were infected for 48 hours with viruses that had 200 ng/mL of p24 Gag antigen, giving a multiplicity of infection (MOI) of 0.7.

Immunostaining. Immunostaining was carried out as described (9). A rabbit polyclonal Rad51 antibody raised against the bacterially expressed protein and a mouse monoclonal antibody raised against synthesized peptides of full-length of Vpr (mAb8D1) were used as the primary antibody. Goat anti-rabbit IgG conjugated with Alexa Fluor 488 (Molecular Probes, Inc., Eugene, OR) and goat anti-mouse IgG conjugated with Cy3 (Zymed Laboratories, Inc., San Francisco, CA) were used as the secondary antibodies. Images were captured on a phase contrast microscope, BX50 (Olympus Corp., Tokyo Japan), or a Radiance 2100 laser scanning confocal microscope (Carl Zeiss, Oberkochen, Germany).

Overexpression and purification of Vpr and its mutant. The HIV-1 *vpr* gene was ligated into the *Nde*I and *Bam*HI sites of the pET15b vector (Novagen, Madison, WI). The Vpr protein and VprΔC12 mutant were produced in the *Escherichia coli* BL21 (DE3) Codon(+)RIL strain (Novagen) by induction with isopropyl-β-D-thiogalactopyranoside (IPTG; Nacalai Tesque, Inc., Kyoto, Japan) and were purified as described in Supplementary Method. The concentration of the purified Vpr protein was determined with a Bio-Rad protein assay kit (Bio-Rad Laboratories, Hercules, CA) using bovine serum albumin (BSA) as the standard.

Isolation of nuclei. Cells scraped from culture dishes were washed once with ice-cold PBS and resuspended in 3 mL of ice-cold 20 mmol/L Tris-HCl buffer (pH 7.6) containing 60 mmol/L KCl, 15 mmol/L NaCl, 5 mmol/L MgCl₂, 1 mmol/L DTT, 250 mmol/L sucrose, 0.6% NP40, and

Note: Supplementary data for this article are available at Cancer Research Online (<http://cancerres.aacrjournals.org/>).

Requests for reprints: Hitoshi Kurumizaka, Graduate School of Science and Engineering, Waseda University, 3-4-1 Okubo, Shinjuku-ku, 169-8555 Tokyo, Japan. Phone: 81-3-5286-8189; Fax: 81-3-5292-9211; E-mail: kurumizaka@waseda.jp and Yukihito Ishizaka, Department of Intractable Diseases, International Medical Center of Japan, 1-21-1 Toyama, Shinjuku-ku, 162-8655 Tokyo, Japan. Phone: 81-3-5272-7527; E-mail: zakay@riimcj.go.jp.

©2006 American Association for Cancer Research.

doi:10.1158/0008-5472.CAN-05-3144

protease inhibitor mixture (Sigma). The cell suspension was incubated for 10 minutes on ice and the sucrose concentration was adjusted to 1.6 mol/L. Then, the sample was loaded onto a sucrose cushion of 2.3 mol/L sucrose solution and centrifuged at $35,000 \times g$ for 30 minutes. The isolated nuclei were obtained in the 2.3 mol/L sucrose fraction. For immunostaining, isolated nuclei were cytocentrifuged to the MAS-coated slide glass (Matsunami Glass IND., LTD., Tokyo, Japan) for 6 minutes at 800 rpm (Thermo Shandon, Chadwick Road, United Kingdom).

PFGE assay. Isolated nuclei were incubated with 10 $\mu\text{mol/L}$ of purified Vpr or Vpr ΔC12 for 15 hours at 30°C. The cells (isolated nuclei) were embedded in agarose plugs at a density of 3×10^5 cells/100 μL . The plugs were treated with proteinase K solution [0.5 mol/L EDTA (pH 8.0), 1% sarcosyl, and 0.5 mg/mL proteinase K] for 38 hours at 50°C. After PFGE was done in a CHEFF Mapper (Bio-Rad Laboratories), the gels were stained with VisTra Green (Amersham Bioscience, Piscataway, NJ).

The DNA-binding assay. The Vpr protein was incubated with ϕX174 single-stranded DNA (ssDNA; 20 $\mu\text{mol/L}$) or ϕX174 superhelical dsDNA (10 $\mu\text{mol/L}$) in 10 μL of 8 mmol/L Tris-HCl buffer (pH 8.5) containing 1 mmol/L DTT and 100 $\mu\text{g/mL}$ BSA. The reaction mixtures were incubated for 1 hour at 37°C and were analyzed by electrophoresis on a 0.8% agarose gel in $1 \times$ TAE buffer (40 mmol/L Tris acetate and 1 mmol/L EDTA) at 3.3 V/cm for 2 hours. The bands were visualized using ethidium bromide staining.

Nuclease activity. The Vpr protein (18.8 $\mu\text{mol/L}$) or DNaseI (Invitrogen Corporation, Carlsbad, CA; 0.02 unit/ μL) were incubated with ϕX174 superhelical double-stranded DNA (dsDNA; 2.5 $\mu\text{mol/L}$) in 40 μL of 15 mmol/L Tris-HCl buffer (pH 8.5) containing 1 mmol/L DTT and 100 $\mu\text{g/mL}$ BSA, in the presence of 5 mmol/L MgCl_2 , MnCl_2 , ZnSO_4 , or CaCl_2 . The reaction mixtures were incubated at 37°C for 30 minutes. After incubation, the samples were treated with proteinase K (0.3 mg/mL) in the presence of 0.1% SDS and the DNA was extracted using phenol-chloroform. The DNA was precipitated by ethanol and was analyzed by electrophoresis on a 0.8% agarose gel in $1 \times$ TAE buffer at 6.6 V/cm for 30 minutes. The bands were visualized with ethidium bromide staining.

The Ni-NTA agarose pull-down assay. Isolated nuclei were disrupted in 20 mmol/L Tris-HCl buffer (pH 8.5) containing 200 mmol/L KCl, 2 mmol/L 2-mercaptoethanol, 0.25 mmol/L EDTA, and 10% glycerol. The extract was incubated with His₆-Vpr (53 $\mu\text{mol/L}$) for 15 hours at 30°C. After incubation, His₆-Vpr was precipitated with 4 μL of Ni-NTA agarose beads and the beads were washed thrice with 500 μL of 20 mmol/L Tris-HCl buffer (pH 7.6) containing 100 mmol/L NaCl, 5 mmol/L DTT, 10 mmol/L imidazole, 1 mmol/L EDTA, and 0.2% Tween 20. The proteins precipitated with the Ni-NTA beads were analyzed by 16% SDS-PAGE. The bands were visualized by silver staining.

Results

Vpr expression induces chromosomal double-strand breaks.

To test whether HIV-1 infection causes double-strand breaks, we used PFGE, which was able to clearly detect the double-strand breaks induced by X-ray irradiation (Fig. 1A, lane 2; ref. 12). HT1080 cells were infected with HIV-1 that had 200 ng/mL of p24 Gag antigen, giving a MOI of 0.7, and the cellular DNA was fractionated using PFGE. Figure 1A (lane 6) shows that HIV-1 infection induced double-strand breaks. Interestingly, the amount of HIV-1-dependent double-strand breaks was reduced significantly (Fig. 1A, lane 5) when the *vpr* gene was deleted from the HIV-1 viral genome (HIV-1 ΔVpr). To show that HIV-1-dependent double-strand breaks are attributable to Vpr expression, we examined double-strand break formation in Vpr stable transfectant, MIT-23 (9), in which Vpr expression is controlled by the *rtet* promoter by doxycycline, and, in ΔVpr , a mock transfectant. As shown in Fig. 1B, double-strand breaks were observed in the Vpr-expressing cells (lane 5, arrow) but not in the mock transfectants (lane 4). Furthermore, Rad51 foci, which are formed

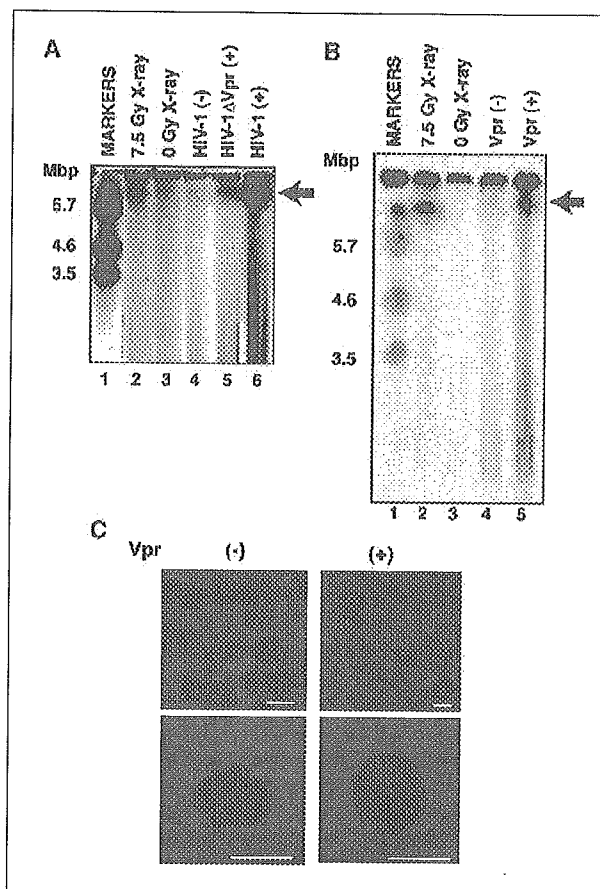


Figure 1. Vpr induces double-strand breaks *in vivo*. **A**, PFGE analysis of double-strand breaks after HIV-1 infection. HT1080 cells were infected with the same amount of HIV-1 or HIV-1 ΔVpr (MOI = 0.7) and subjected to PFGE. As a positive control, uninfected cells were analyzed immediately after 7.5 Gy of X-ray irradiation. Molecular mass markers (lane 1), control cells (lanes 3 and 4), cells subjected to X-ray irradiation (lane 2), and cells infected with HIV-1 ΔVpr (lane 5) or HIV-1 (lane 6) are shown. Arrow, position corresponding to the double-strand breaks. **B**, PFGE analysis in Vpr-expressing cells. Molecular mass markers (lane 1), cells irradiated with 7.5 Gy (lane 2), control cells (lane 3), mock transfectants (lane 4), and cells with Vpr expression (lane 5) are shown. Arrow, double-strand breaks. **C**, Rad51 focus formation with Vpr expression. An immunohistochemical analysis was used to detect Rad51 in cells with (right) or without (left) Vpr expression. Bar, 10 μm .

at double-strand break sites (13), were observed with Vpr expression (Fig. 1C). These results indicate that Vpr is responsible for double-strand break formation. The double-strand breaks shown in Fig. 1B were not the result of an apoptotic process as the DNA ladder typically observed in apoptotic cells (14) was not detected (data not shown).

Vpr has no endonuclease activity. Next, we studied whether Vpr directly induces double-strand breaks. The recombinant Vpr protein was purified to near homogeneity (Fig. 2A) and the DNA-binding activity of Vpr was examined. As shown in Fig. 2B, purified Vpr bound both ssDNA (lanes 2-6) and dsDNA (lanes 8-12) in an ATP- and Mg^{2+} -independent manner (15). Then, we examined whether Vpr has nuclease activity. Superhelical dsDNA containing small amounts of nicked circular dsDNA was incubated with Vpr in the presence of various divalent cations. After the incubation, the proteins were removed and the DNA was examined by

electrophoresis. If Vpr induces a double-strand break or nick, the superhelical dsDNA would give rise to linear or nicked circular forms, producing a different electrophoretic pattern. However, the DNA incubated with Vpr in the absence (*lane 2*) or presence of any divalent cation examined (*lanes 4, 6, 8, and 10*) showed the same migration pattern with control (*lane 1*), indicating that Vpr does not cleave DNA (Fig. 2C). Positive control experiments showed that the DNA was digested by DNaseI with MgCl₂, MnCl₂, or CaCl₂ (*lanes 5, 7, and 11*) but not with ZnSO₄ (*lane 9*; Fig. 2C). Therefore, these results indicate that Vpr lacks endonuclease or nicking activity.

Vpr induces double-strand breaks *in vitro*. In a second approach, we tested whether purified Vpr induces double-strand breaks in nuclei isolated from HT1080 cells (Fig. 3A). First, we confirmed by a laser confocal microscopy that Vpr localizes in nuclei after incubation *in vitro* (Fig. 3B). The nuclear DNA was then analyzed for double-strand breaks by using PFGE (Fig. 3C). Interestingly, purified Vpr induced double-strand breaks in the DNA of the isolated nuclei (Fig. 3C, *lane 5, arrow*). By contrast, few double-strand breaks were detected without Vpr (Fig. 3C, *lane 4*). Because Vpr alone did not show endonuclease activity (Fig. 2C), these results suggest that Vpr interacts with intrinsic nuclear protein(s), which required for double-strand break formation. To identify candidates for the Vpr-interacting nuclear proteins, we did the Ni-NTA pull-down assay. In this assay, recombinant His₆-tagged Vpr was incubated with the extract from isolated nuclei and Ni-NTA beads precipitated proteins bound to His₆-tagged Vpr (Fig. 3D). As shown in Fig. 3D, His₆-tagged Vpr associated with numerous proteins that were not detected in the control precipitates (*lane 2, asterisks*).

The DNA-binding activity of Vpr is correlated with double-strand break formation. The COOH-terminal region of Vpr is arginine rich and is thought to be an important site for DNA binding to Vpr (15). Nuclear magnetic resonance analysis shows that Vpr has three α -helices (amino acids 17-33, 38-50, and 56-77)

in solution, whereas the COOH-terminal region from amino acid residues 84 to 96 is disordered (16). This suggests that the deletion of the COOH-terminal 12 amino acid residues does not affect the tertiary structure of Vpr. We purified a Vpr mutant protein lacking the COOH-terminal 12-amino-acid residues (Vpr Δ C12; Fig. 4A), and examined its DNA-binding activity. Purified Vpr Δ C12 was significantly defective in both ssDNA- and dsDNA-binding activity compared with wild-type Vpr (Fig. 4B). Interestingly, Vpr Δ C12 induced double-strand breaks in isolated nuclei but its efficiency was reduced significantly (Fig. 4C, *lane 6*). These results indicate that the DNA-binding ability of Vpr is important for the induction of double-strand breaks by Vpr.

Discussion

Here, we present evidence that HIV-1 Vpr induces double-strand breaks. Our data are consistent with previous observations in Vpr-expressing cells: the up-regulation of gene amplification events that are believed to be introduced by broken DNA strands (17) and the activation of activating Rad3-related/ataxia-telangiectasia mutated, followed by the phosphorylation of their downstream substrate, a histone H2A variant, H2AX, and γ -H2AX and BRCA1 focus formation (8). Biochemical analyses using purified Vpr indicated that Vpr alone has no endonuclease activity (Fig. 2C), suggesting that a cellular factor(s), possibly with endonuclease activity, is required for Vpr-dependent double-strand breaks. The factor(s) required for double-strand breaks must preexist in nuclei because double-strand breaks were observed upon incubating a mixture of isolated nuclei and purified Vpr *in vitro* (Fig. 3C). As one possible mechanism, Vpr may recruit a nuclease factor to chromosomal DNA, given that the Vpr-dependent double-strand breaks were correlated with the DNA-binding activity (Figs. 4B and C). Alternatively, Vpr itself may acquire endonuclease activity after modification in the nucleus. Further analyses are necessary to clarify this point.

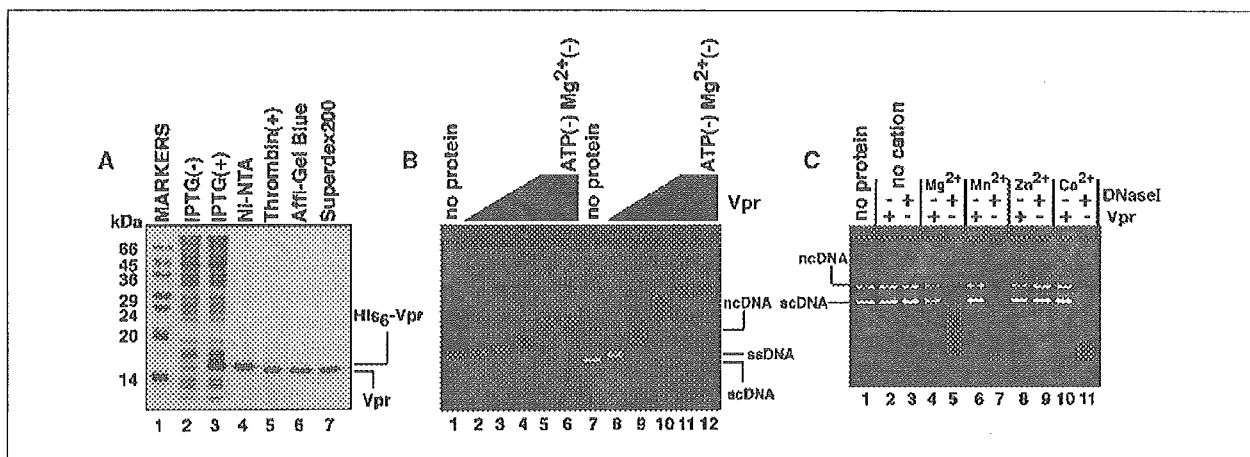


Figure 2. The Vpr-DNA interaction *in vitro*. *A*, purification of recombinant Vpr. Proteins from each purification step were analyzed using 16% SDS-PAGE with Coomassie brilliant blue staining. Molecular mass markers (*lane 1*), whole-cell lysates before (*lane 2*) and after (*lane 3*) induction with IPTG, samples from the Ni-NTA fraction (*lane 4*), the fraction after removing the hexahistidine tag (*lane 5*), the Affi-Gel Blue fraction (*lane 6*), and the Superdex 200 fraction (*lane 7*) are shown. *B*, the DNA-binding activity of Vpr. ϕ X174 circular ssDNA (20 μ mol/L; *lanes 2-6*) and ϕ X174 superhelical dsDNA (scDNA; 10 μ mol/L; *lanes 8-12*) containing a small amount of nicked circular DNA (ncDNA) were incubated with Vpr in the presence of 1 mmol/L ATP and 1 mmol/L MgCl₂. Control experiments without ATP and MgCl₂ (*lanes 6 and 12*) are included. The Vpr concentrations were 1.25 μ mol/L (*lanes 2 and 8*), 2.5 μ mol/L (*lanes 3 and 9*), 5 μ mol/L (*lanes 4 and 10*), and 10 μ mol/L (*lanes 5, 6, 11, and 12*). *Lanes 1 and 7*, negative controls without protein. *C*, nuclease activity. ϕ X174 scDNA (2.5 μ mol/L) was incubated with Vpr (18.8 μ mol/L; *lanes 2, 4, 6, 8, and 10*) or DNaseI (*lanes 3, 5, 7, 9, and 11*) in the absence of divalent cation (*lanes 2 and 3*) or in the presence of 5 mmol/L MgCl₂ (*lanes 4 and 5*), 5 mmol/L MnCl₂ (*lanes 6 and 7*), 5 mmol/L ZnSO₄ (*lanes 8 and 9*), or 5 mmol/L CaCl₂ (*lanes 10 and 11*). *Lane 1*, negative control without protein.

In the HIV-1 life cycle, DNA breakage and repair are thought to be essential steps for integrating the double-stranded viral cDNA into the host genome. In this study, we found that Vpr is one molecule responsible for the double-strand breaks that occur upon HIV-1 infection. However, it is also noteworthy that some double-strand breaks were induced in the cells with HIV-1ΔVpr (Fig. 1A, lane 5), suggesting that other viral factors are also involved. It has been shown that integrase activates the ataxia-telangiectasia mutated-dependent pathway (7) and, thus, the double-strand breaks observed with HIV-1ΔVpr infection are probably owing to integrase. For viral integration to occur, the amount of double-strand breaks induced by HIV-1ΔVpr (Fig. 1A, lane 5) may be sufficient, because viral production in peripheral blood mononuclear cells was not alleviated by infection with

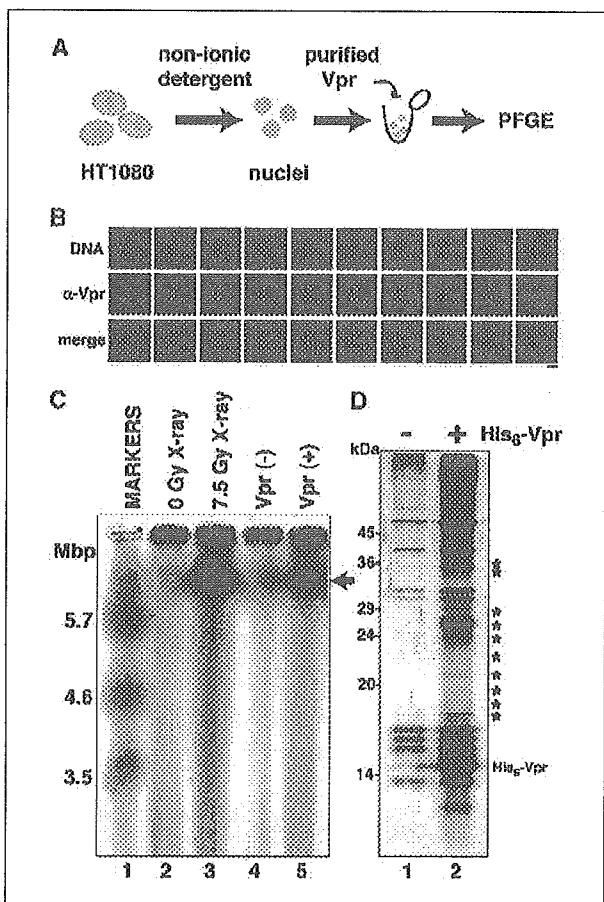


Figure 3. Purified Vpr induces double-strand breaks *in vitro*. *A*, a scheme of the protocol used to detect Vpr-induced double-strand breaks in isolated nuclei. *B*, Vpr localization in isolated nuclei. Isolated nuclei from HT1080 after incubation with Vpr were immunostained by α -Vpr (mAb8D1) and the images were captured by a laser confocal microscopy. The Z-series of optical sections collected at 1 μ m steps of the cells were presented. Vpr (red; middle), DNA staining by Hoechst (blue; top) and their merged images (bottom) are shown. Without Vpr incubation, any signals by α -Vpr immunostaining were not detected in isolated nuclei (data not shown). Bar, 10 μ m. *C*, PFGE analysis of double-strand breaks in isolated nuclei treated with Vpr. Molecular mass markers (lane 1), control cells (lane 2), cells subjected to X-ray irradiation (lane 3), and isolated nuclei without (lane 4) or with 10 μ mol/L Vpr (lane 5). Arrow, double-strand breaks. *D*, Ni-NTA pull-down assay with His₆-tagged Vpr on isolated nuclei. Precipitated proteins bound to His₆-tagged Vpr (lane 2) and the control precipitates (lane 1) are indicated. *, His₆-Vpr-specific bands.

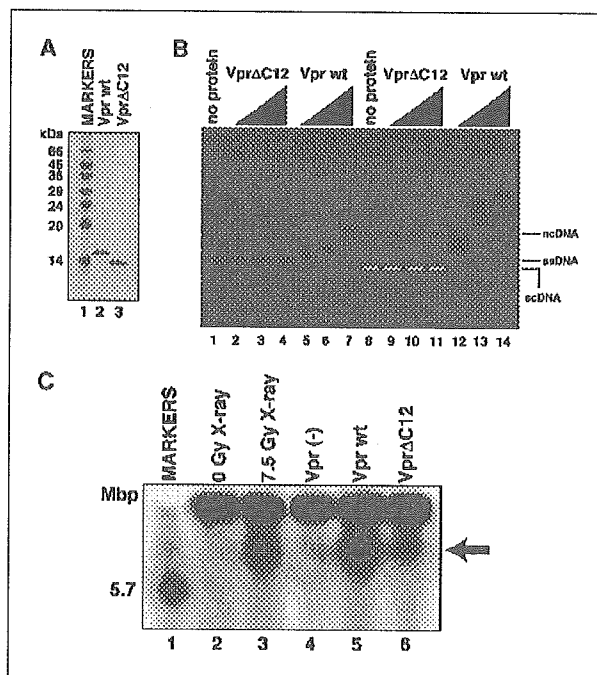


Figure 4. DNA-binding and double-strand break formation by Vpr. *A*, purification of Vpr Δ C12. Purified Vpr Δ C12 was analyzed using 16% SDS-PAGE with Coomassie brilliant blue staining. Lane 1, molecular mass markers. Lanes 2 and 3, purified wild-type Vpr and Vpr Δ C12 protein, respectively. *B*, the DNA-binding activity of Vpr Δ C12. The DNA-binding experiments were done using the protocol used to obtain Fig. 2B. The concentrations of Vpr Δ C12 were 2.5 μ mol/L (lanes 2 and 9), 5 μ mol/L (lanes 3 and 10), and 10 μ mol/L (lanes 4 and 11), and those of the wild-type Vpr were 2.5 μ mol/L (lanes 5 and 12), 5 μ mol/L (lanes 6 and 13), and 10 μ mol/L (lanes 7 and 14). Negative controls without protein (lanes 1 and 8) are included. *C*, PFGE analysis of double-strand breaks in isolated nuclei treated with Vpr or Vpr Δ C12. Molecular mass marker (lane 1), cells without (lane 2) or with (lane 3) 7.5 Gy of X-ray irradiation, control nuclei (lane 4), nuclei with Vpr (lane 5), and nuclei with Vpr Δ C12 (lane 6). Vpr was used at 10 μ mol/L. Arrow, double-strand breaks.

Vpr-deleted HIV-1 (18).⁴ Vpr-induced double-strand breaks may be surplus to those required for viral integration (Fig. 1A, lane 6). The resultant DNA damage may reduce the integrity of the host genome.

Recently, DNA damage signaling was observed at an early stage of tumor development, suggesting that the DNA damage response is a mechanism to prevent the progression of pre-neoplastic lesions (5). If DNA repair is not accomplished correctly or is skipped because of unregulated checkpoint controls, the genomic structure would be altered severely (19). The progression of malignant tumors in AIDS-defining cancers is well documented in oncovirus infections (1, 2). If DNA damage increases the probability of neoplasia, Vpr-induced double-strand breaks with oncovirus infection may accelerate tumor progression during the clinical course of AIDS. In addition to AIDS-defining cancers, non-AIDS-defining cancers also occur at a higher incidence and the factor responsible for such oncogenesis is now a critical issue (3, 4). Vpr-induced DNA damage may result in

⁴ M. Shimura, unpublished data.

these AIDS-related malignancies. It is essential to explore the molecular mechanism of Vpr-induced double-strand breaks to clarify their role in HIV-1 infection and their effect on the stability of the host cell genome.

Acknowledgments

Received 9/1/2005; revised 11/16/2005; accepted 11/22/2005.

Grant support: Grants-in-Aid for Scientific Research from the Ministry of Health, Labor, and Welfare of Japan; the Japanese Society for the Promotion of Science; the Ministry of Education, Sports, Culture, Science, and Technology of Japan; and a research grant from the Kato Memorial Trust for Nambyo Research and the Japan Health Sciences Foundation.

The costs of publication of this article were defrayed in part by the payment of page charges. This article must therefore be hereby marked *advertisement* in accordance with 18 U.S.C. Section 1734 solely to indicate this fact.

We thank Dr. Masashi Tatsumi (National Institute of Infectious Diseases, Tokyo, Japan) for providing us with MAGIC5 cells and Koji Nakatani for his technical assistance and heart-warming support.

References

- Beral V, Peterman T, Berkelman R, Jaffe H. AIDS-associated non-Hodgkin lymphoma. *Lancet* 1991;337:805-9.
- Bellan C, De Falco G, Lazzi S, Leoncini L. Pathologic aspects of AIDS malignancies. *Oncogene* 2003;22:6639-45.
- Wistuba II, Behrens C, Gazdar AF. Pathogenesis of non-AIDS-defining cancers: a review. *AIDS Patient Care STDS* 1999;13:415-26.
- Chiao EY, Krown SE. Update on non-acquired immunodeficiency syndrome-defining malignancies. *Curr Opin Oncol* 2003;15:389-97.
- Bartkova J, Horejsi Z, Koed K, et al. DNA damage response as a candidate anti-cancer barrier in early human tumorigenesis. *Nature* 2005;434:864-70.
- Gorgoulis VG, Vassiliou L-VF, Karakaidos P, et al. Activation of the DNA damage checkpoint and genomic instability in human precancerous lesions. *Nature* 2005;434:907-13.
- Lau A, Swinbank KM, Ahmed PS, et al. Suppression of HIV-1 infection by a small molecule inhibitor of the ATM kinase. *Nat Cell Biol* 2005;7:493-500.
- Zimmerman ES, Chen J, Andersen JL, et al. Human immunodeficiency virus type 1 Vpr-mediated G₂ arrest requires Rad17 and Hus1 and induces nuclear BRCA1 and γ -H2AX focus formation. *Mol Cell Biol* 2004;24:9286-94.
- Shimura M, Tanaka Y, Nakamura S, et al. Micronuclei formation and aneuploidy induced by Vpr, an accessory gene of human immunodeficiency virus type 1. *FASEB J* 1999;13:621-37.
- Adachi A, Gendelman HE, Koenig S, et al. Production of acquired immunodeficiency syndrome-associated retrovirus in human and nonhuman cells transfected with an infectious molecular clone. *J Virol* 1986;59:284-91.
- Tokunaga K, Greenberg ML, Morse MA, Cumming RI, Lysterly HK, Cullen BR. Molecular basis for cell tropism of CXCR4-dependent human immunodeficiency virus type 1 isolates. *J Virol* 2001;75:6776-85.
- Kruger I, Rothkamm K, Löbrich M. Enhanced fidelity for rejoining radiation-induced DNA double-strand breaks in the G₂ phase of Chinese hamster ovary cells. *Nucleic Acids Res* 2004;32:2677-84.
- Haaf T, Golub EI, Reddy G, Radding CM, Ward DC. Nuclear foci of mammalian Rad51 recombination protein in somatic cells after DNA damage and its localization in synaptonemal complexes. *Proc Natl Acad Sci U S A* 1995;92:2298-302.
- Maecker HT, Hedjbeli S, Alzona M, Le PT. Comparison of apoptosis signaling through T cell receptor, fas, and calcium ionophore. *Exp Cell Res* 1996;222:95-102.
- Zhang S, Pointer D, Singer G, Feng Y, Park K, Zhao LJ. Direct binding to nucleic acids by Vpr of human immunodeficiency virus type 1. *Gene* 1998;212:157-66.
- Morellet N, Bouaziz S, Petitjean P, Roques BP. NMR structure of the HIV-1 regulatory protein VPR. *J Mol Biol* 2003;327:215-27.
- Shimura M, Onozuka Y, Yamaguchi T, Hatake K, Takaku F, Ishizaka Y. Micronuclei formation with chromosome breaks and gene amplification caused by Vpr, an accessory gene of human immunodeficiency virus. *Cancer Res* 1999;59:2259-64.
- Kawano Y, Tanaka Y, Misawa N, et al. Mutational analysis of human immunodeficiency virus type 1 (HIV-1) accessory genes: requirement of a site in the nef gene for HIV-1 replication in activated CD4⁺ T cells *in vitro* and *in vivo*. *J Virol* 1997;71:8456-66.
- Furuta S, Jiang X, Gu B, Cheng E, Chen PL, Lee WH. Depletion of BRCA1 impairs differentiation but enhances proliferation of mammary epithelial cells. *Proc Natl Acad Sci U S A* 2005;102:9176-81.

compared with four in the experienced group. Four of these five patients had HCV co-infection. Two events arose after one month of treatment and the other three after a year, confirming the multifaceted mechanisms causing this toxicity. In all these cases the treatment had to be stopped, and the patients regressed.

To the best of our knowledge, this study comprises the biggest series to date of patients treated with lopinavir/ritonavir and followed prospectively outside clinical trials. In addition, this HIV-positive population had a high prevalence of co-infection with hepatitis viruses.

The frequency of hepatotoxicity was actually low, unlike in other studies. This might partly be the result of methodological differences, reflecting how the data were collected. Retrospective studies can suffer major selection bias. Gonzalez-Requena *et al.* [11] also reported a low incidence of adverse events, but their case series was small and was followed up for not more than one year.

In conclusion, the present study found that lopinavir/ritonavir caused only limited hepatic toxicity in this population of HIV-positive patients with a high prevalence of co-infection with hepatitis B virus or HCV.

The CISA Study Group

Coordination: T. Quirino, P. Bonfanti, G.M. Vigevani, F. Parazzini, E. Ricci

Recruitment sites and investigators: R. Cinelli, U. Tirelli (Aviano); G. Cocca, G. Rizzardini (Busto Arsizio); C. Grosso, A. Stagno (Cesena); L. Pusterla, D. Santoro (Como); C. Magnani, P. Viganò (Cuggiono); S. Carradori, F. Ghinelli (Ferrara); F. Vichi, F. Mazzotta (Firenze, S. Maria Annunziata); C. Martinelli, F. Leoncini (Firenze, Careggi); G. Penco, G. Cassola (Genova); S. Miccolis, A. Scalzini (Mantova); S. Landonio, M. (I Divisione, Ospedale Sacco, Milano); L. Valsecchi, L. Cordier, A. Cargnel (II Divisione, Ospedale Sacco, Milano); T. Bini, S. Melzi, M. Moroni (Clinica Malattie Infettive, Ospedale Sacco, Milano); E. Rosella, G. Fioni (Milano); M. Gargiulo, A. Chirianni (Napoli); M. Franzetti, P. Cadrobbi (Padova); C. Sfara, G. Stagni (Perugia); G. Parruti, G. Marani Toro (Pescara); B. Adriani, A. Paladini (Prato); G. Madeddu, M.S. Mura (Sassari); G. Liuzzi, A. Antinori (Roma); G. Orofino, P. Caramello (Torino); G. Cristina, F. Carcò (Vercelli); D. Migliorini, O. Armignacco (Viterbo).

^a*Divisione di Malattie Infettive, Ospedale Luigi Sacco, Milan, Italy;* ^b*Divisione di Malattie Infettive, Ospedale Galliera, Genoa, Italy;* ^c*Divisione A di Malattie Infettive, Ospedale Amedeo di Savoia, Turin, Italy;* ^d*Clinica di Malattie Infettive, Ospedale Luigi Sacco, Milan, Italy;* ^e*Clinica di Malattie Infettive, Perugia, Italy;* ^f*Divisione di Malattie Infettive, Cremona, Italy;*

^g*Divisione di Malattie Infettive, Vercelli, Italy;* and ^h*Divisione di Malattie Infettive, Busto Arsizio, Italy.*

Sponsorship: This study was supported by a grant from the Istituto Superiore di Sanità (5th National Research Program on AIDS, no. 30F.43), Rome.

Received: 23 May 2005; accepted: 21 June 2005.

References

1. Wit FWNM, Weverling CJ, Weel J, Jurriens S, Lange JMA. **Incidence and risk factors for severe hepatotoxicity associated with antiretroviral combination therapy.** *J Infect Dis* 2002; **186**:23–31.
2. Puoti M, Torti C, Ripamonti D, and the HIV/HCV Co-infection Study Group. **Severe hepatotoxicity during combination antiretroviral treatment: incidence, liver histology, and outcome.** *J Acquir Immune Defic Syndr* 2003; **32**:259–267.
3. Sulkowski MS, Mast EE, Seeff LB, Thomas DL. **Hepatitis C virus infection as an opportunistic disease in persons infected with human immunodeficiency virus.** *Clin Infect Dis* 2000; **30** (Suppl. 1):S77–S84.
4. Bonfanti P, Landonio S, Ricci E, Martinelli C, Fortuna P, Faggion I, *et al.* **Risk factors for hepatotoxicity in patients treated with highly active antiretroviral therapy.** *J Acquir Immune Defic Syndr* 2001; **27**:316–318.
5. Martinez E, Blanco JL, Arnaiz JA, Perez-Cuevas JB, Mocroft A, Cruceta A, *et al.* **Hepatotoxicity in HIV-1 infected patients receiving nevirapine-containing antiretroviral therapy.** *AIDS* 2001; **15**:1261–1268.
6. Hicks C, King MS, Gulick R, Clinton White A, Eron JJ, Kessler HA, *et al.* **Long-term safety and durable antiretroviral activity of lopinavir/ritonavir in treatment-naïve patients: 4-year follow-up study.** *AIDS* 2004; **18**:775–779.
7. Sulkowski MS, Mehta SH, Chaisson RE, Thomas DL, Moore RD. **Hepatotoxicity associated with protease inhibitor-based antiretroviral regimens with or without concurrent ritonavir.** *AIDS* 2004; **18**:2277–2284.
8. Meraviglia P, Schiavini M, Castagna A, Viganò P, Bini T, Landonio S, *et al.* **Lopinavir/ritonavir treatment in HIV antiretroviral-experienced patients: evaluation of risk factors for liver enzyme elevation.** *HIV Med* 2004; **5**:334–343.
9. Bonfanti P, Martinelli C, Ricci E, Carradori S, Parruti G, Armignacco O, *et al.* **An Italian approach to post-marketing monitoring: preliminary results from the SCOLTA Project on the safety of lopinavir/ritonavir.** *J Acquir Immune Defic Syndr* 2005; **39**:317–320.
10. AIDS Clinical Trials Group. *Table of grading severity of adult severe experiences.* Rockville: Division of AIDS, National Institute of Allergy and Infectious Diseases. 1996.
11. Gonzalez-Requena D, Nunez M, Jimenez-Nacher I, Gonzalez-Lahoz J, Soriano V. **Short communication: liver toxicity of lopinavir-containing regimens in HIV-infected patients with or without hepatitis C co-infection.** *AIDS Res Hum Retroviruses* 2004; **20**:698–700.

Premature sister chromatid separation in HIV-1-infected peripheral blood lymphocytes

Mari Shimura^a, Kenzo Tokunaga^b, Mitsuru Konishi^c, Yuko Sato^d, Chizuko Kobayashi^e, Tetsutaro Sata^b and Yukihito Ishizaka^a

To investigate the mechanism of aneuploidy that is frequently observed in AIDS, we examined premature sister chromatid separation (PCS), a sign of genomic instability, in peripheral blood cells of HIV-1-infected individuals. PCS was found in all

six HIV-1 individuals at a high incidence. When peripheral blood cells from healthy volunteers were infected with HIV-1 *in vitro*, the incidence of PCS increased. This suggests that HIV-1 infection causes PCS and has the potential to induce aneuploidy.

Malignancy in HIV infection influences the prognosis of AIDS patients. These neoplasms are the result of various diseases that accompany immunodeficiency, such as co-infections with Epstein-Barr virus or human herpes virus

8 [1-4]. Besides these AIDS-defining cancers, several non-AIDS-defining cancers also occur at a higher incidence in HIV-infected individuals [5-9]. Moreover, it has been reported that HIV-1 itself is tumorigenic in immortalized B cells in nude mice [10,11]. These reports lead to the hypothesis that HIV-1 has the potential to induce neoplasms before AIDS develops.

Aneuploidy is a phenomenon of chromosome instability that is frequently reported in HIV-1-infected individuals

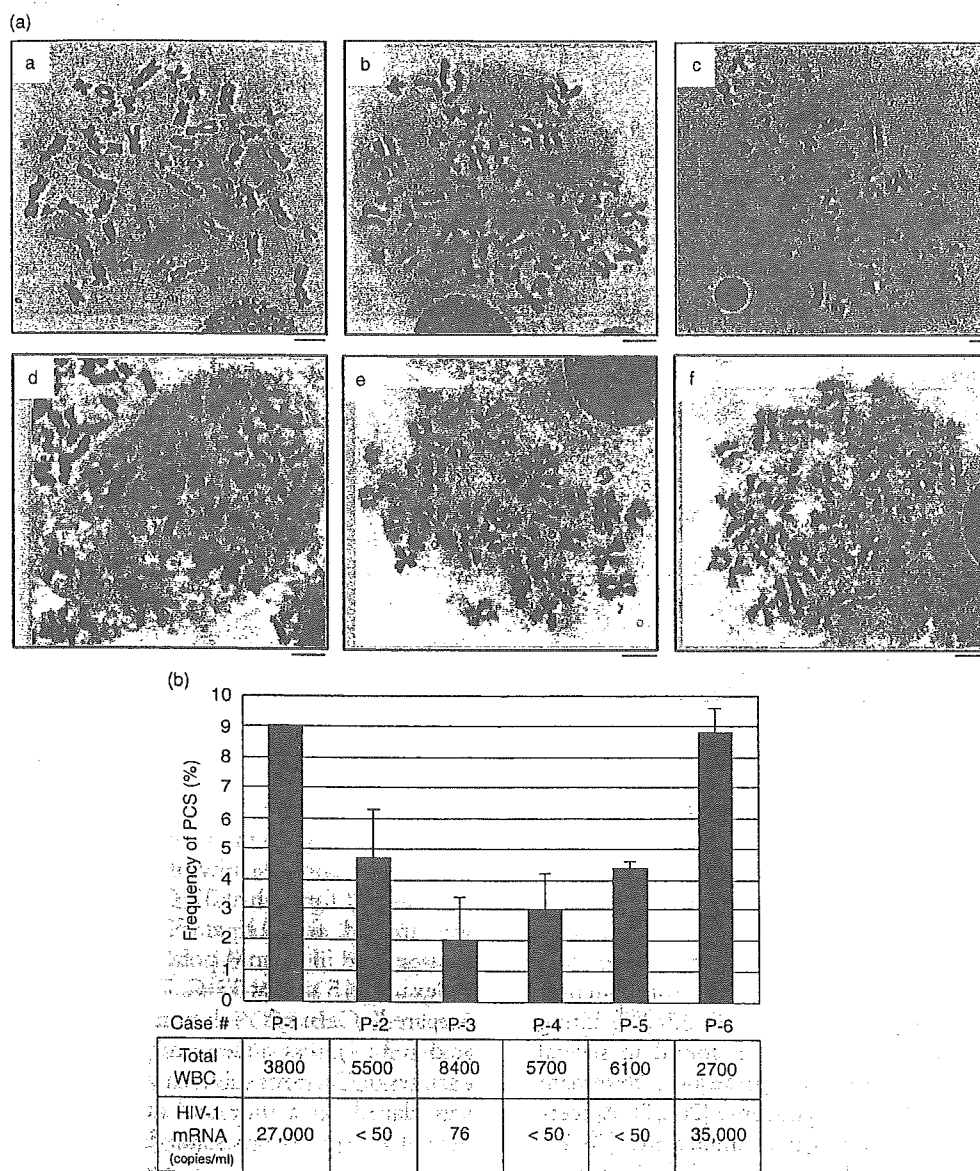


Fig. 1. Metaphase spreads of blood cells in HIV-1 infection. (a) Representative metaphase spreads of peripheral blood cells from HIV-1-infected individuals (b, c, d, e, and f are from cases nos. P-1, 2, 4, 5, and 6, respectively, see Fig. 1b). (a). (b) Frequency of premature sister chromatid separation (PCS). The frequency of PCS (black bar), and number of HIV-1 messenger RNA copies and total white blood cells (WBC) are shown. (c) Metaphase spreads of peripheral blood mononuclear cells (PBMC) from healthy volunteers. Representative metaphase spreads of PBMC from healthy volunteers with (a/+, b/+, and c/+) or without (a, b, and c) vesicular stomatitis virus G protein (VSV-G)-pseudotyped HIV-1 infection are shown. (d) Aneuploidy in HIV-1-infected cells. Metaphase spreads from P-1, P-6 and from PBMC with VSV-G-pseudotyped HIV-1 infection were positive for aneuploidy with numbers of chromosomes of 85, 75 and 65, respectively. The scale bar represents 5 μ m.

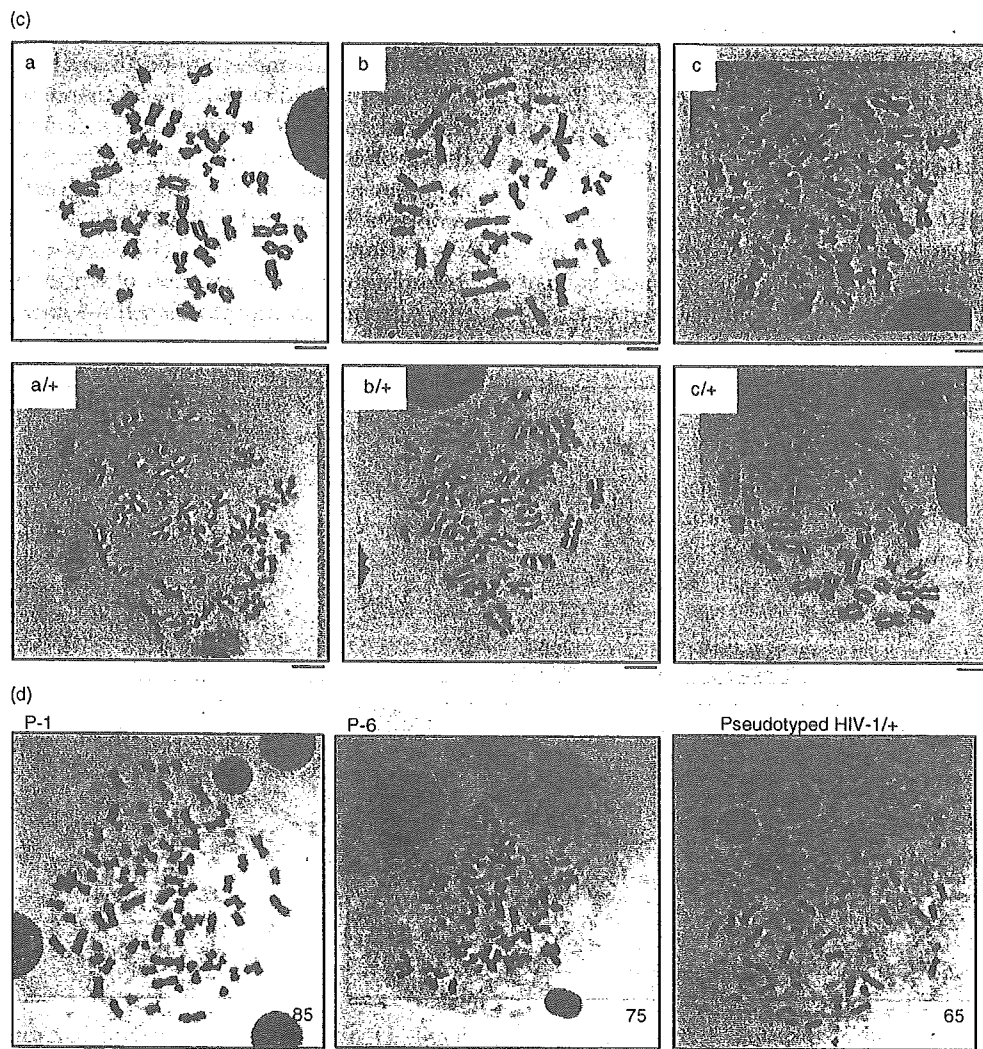


Fig. 1. (continued)

[12–14]. One of the major factors accelerating aneuploidy is thought to be abnormal chromatid separation [15–17]. At metaphase, paired sister chromatids are folded at the centric region until the onset of anaphase [18–22]. If the attachment of the sister chromatids is abolished before the onset of anaphase, premature sister chromatid separation (PCS) occurs. Subsequently, chromosome mis-segregation is induced, often resulting in aneuploidy [16,17]. PCS has been found in several clinical conditions, including aging, familial dominant inheritance [23–25], Roberts syndrome [26,27], cancer-prone syndrome mosaic variegated aneuploidy [28,29] and general tumours [30,31]. Note that all of these cases of PCS are associated with aneuploidy, indicating that a high PCS rate is a sign of chromosome instability. To investigate the cellular mechanism of HIV-1-related aneuploidy, we examined PCS in peripheral blood cells of HIV-1-infected individuals.

Peripheral blood was collected in sodium heparin (20 U/ml) from HIV-1-infected patients or healthy

volunteers. We added 0.5 ml whole blood to 9.5 ml RPMI-1640 growth medium containing 10% fetal calf serum and 2% phytohemagglutinin M-form, and incubated it for 82 h at 37°C. Then colcemid (30 ng/ml) was treated for 2 h at 37°C. Recovered cells were resuspended in 75 mM potassium chloride and incubated for exactly 15 min at 37°C. To the cell suspension, freshly prepared Carnoy's solution (methanol:glacial acetic acid = 3 : 1) was added and mixed gently. After three changes of Carnoy's solution, a drop of the cell suspension was placed on a slide and air dried. Subsequently, the metaphase spread was stained with Giemsa.

Surprisingly, the HIV-1 patients examined showed PCS at high frequencies of 2.1 to 9.0% (mean \pm standard deviation; $5.36 \pm 2.92\%$; Fig. 1a, panels b–f and Fig. 1b). A high incidence of PCS was observed in HIV-1-infected individuals with high viral RNA copy numbers (Fig. 1b), in which total PCS was often observed (patient case no. 1 and no. 6; panels b and f). By contrast, peripheral blood mononuclear cells (PBMC) from healthy volunteers

showed normal attachments at the centromere (Fig. 1a, panel a), and PCS was detected in less than 2% ($1.22 \pm 0.48\%$).

We next clarified whether the PCS was attributable to HIV-1 infection. The PBMC (1.5×10^6) [32] were infected with vesicular stomatitis virus G protein (VSV-G)-pseudotyped HIV-1 [33] at the concentration of 2 ng/ml of p24 Gag antigen of pseudotyped virus (multiplicity of infection at 0.007). They were incubated for 82 h in the presence of 2% phytohemagglutinin M-form, and metaphase spread was analysed as described above. All of the specimens from three volunteers showed an increased incidence of PCS after HIV-1 infection (Fig. 1c, lower panels), whereas PCS was barely detectable without infection (Fig. 1c, upper panels). The frequencies of PCS after HIV-1 infection in the three samples were 8.40 ± 1.09 , 5.28 ± 1.40 , and 7.34 ± 1.67 , whereas the frequencies without infection were 1.26 ± 0.40 , 0.72 ± 0.22 , and 1.68 ± 0.86 , respectively. Our present data suggest that HIV-1 infection is a primary factor inducing PCS.

In the patients' case, the frequency of PCS was positively correlated with the reduction in total white blood cells (Pearson product-moment correlation coefficient $r = 0.837$, $P < 0.01$; Fig. 1b) rather than CD4 positive lymphocytes ($r = 0.011$, $P > 0.05$). Although VSV-G-pseudotyped HIV-1 was infected to PBMC at a multiplicity of infection of 0.007 (0.7%), the average incidence of PCS with HIV-1 infection exceeded 7%. Taken together with the information that pseudotyped HIV-1 induces a single round of infection, these data suggest that PCS occurs not only in response to the infection itself but also as a result of the effects of other virus products or cellular proteins stimulated by HIV-1 infection.

Simultaneously, we found aneuploidy in hyperploid cells of HIV-1-infected individuals who had high viral loads and high PCS frequency (Fig. 1b and Fig. 1d, left and middle panels). We also found aneuploidy in PBMC with HIV-1 infection *in vitro* (Fig. 1d, right panel). By contrast, aneuploidy was not found in control PBMC. Although it remains to be determined whether PCS is directly related to neoplasms in AIDS, we speculate that a high incidence of PCS and constitutive virus infection augment the susceptibility of the cells to aneuploidy and may play a critical role in the development of AIDS-related neoplasms. It will be important to track the epidemiological and biological features of the incidence of PCS in HIV-1 infection.

Acknowledgements

The authors would like to thank Dr Masashi Tatsumi for his kind gift of MAGIC5 cells.

Sponsorship: This work was supported by a grant-in-aid for scientific research from the Ministry of Health, Labour and Welfare of Japan, and partly supported by a research grant from the Kato Memorial Trust for Nambyo Research.

This study was approved by the institutional Ethics Committees of Nara Medical University, National Hospital Organization Chiba Medical Center, and the International Medical Center of Japan.

^aDepartment of Intractable Diseases, Research Institute, International Medical Center of Japan, 1-21-1 Toyama, Shinjuku-ku, Tokyo 162-8655, Japan; ^bDepartment of Pathology, National Institute of Infectious Disease, 1-23-1 Toyama, Shinjuku-ku, Tokyo 162-8640, Japan; ^cCenter for Infectious Diseases, Nara Medical University, 840 Shijo-cho, Kashihara, Nara 634-8522, Japan; ^dDepartment of Clinical Pathology, Research Institute, International Medical Center of Japan, 1-21-1 Toyama, Shinjuku-ku, Tokyo 162-8655, Japan; and ^eDepartment of Internal Medicine, National Hospital Organization Chiba Medical Center, 4-1-2 Tsubakimori, Chuo-ku, Chiba 260-8606, Japan.

Received: 19 April 2005; revised: 7 June 2005; accepted: 27 June 2005.

References

- Beral V, Peterman T, Berkelman R, Jaffe H. AIDS-associated non-Hodgkin lymphoma. *Lancet* 1991; **337**:805-809.
- Biggar RJ, Rosenberg PS, Coté T, and the Multistate AIDS/Cancer Match Study Group. Kaposi's sarcoma and non-Hodgkin's lymphoma following the diagnosis of AIDS. *Int J Cancer* 1996; **68**:754-758.
- Flore O, Rafii S, Ely S, O'Leary JJ, Hyjek EM, Cesarman E. Transformation of primary human endothelial cells by Kaposi's sarcoma-associated herpesvirus. *Nature* 1998; **394**:588-592.
- Miklos G. AIDS, aneuploidy and oncogenes. *Nat Biotech* 2004; **22**:1077-1078.
- Wistuba II, Behrens C, Gazdar AF. Pathogenesis of non-AIDS-defining cancers: a review. *AIDS Patient Care STDS* 1999; **13**:415-426.
- Remick SC. Non-AIDS-defining cancers. *Hematol Oncol Clin North Am* 1996; **10**:1203-1213.
- Frisch M, Biggar RJ, Engles EA, Goedert JJ, and the AIDS-cancer match registry study group. Association of cancer with AIDS-related immunosuppression in adults. *JAMA* 2001; **285**:1736-1745.
- Vaccher E, Spina M, Tirelli U. Clinical aspects and management of Hodgkin's disease and other tumors in HIV-infected individuals. *Eur J Cancer* 2001; **37**:1306-1315.
- Chiao EY, Krown SE. Update on non-acquired immunodeficiency syndrome-defining malignancies. *Curr Opin Oncol* 2003; **15**:389-397.
- Laurence J, Astrin SM. Human immunodeficiency virus induction of malignant transformation in human B lymphocytes. *Proc Natl Acad Sci U S A* 1991; **88**:7635-7639.
- Astrin SM, Laurence J. Human immunodeficiency virus activates c-myc and Epstein-Barr virus in human B lymphocytes. *Ann NY Acad Sci* 1992; **651**:422-432.
- Abramson J, Verma RS. Acquired immunodeficiency syndromes and concomitant non-Hodgkin's lymphoma in a patient with new chromosomal abnormality. *Acta Haematol* 1987; **77**:234-237.
- Zunino A, Viaggi S, Ottaggio L, Fronza G, Schenone A, Roncella S, et al. Chromosomal aberrations evaluated by CGH, FISH and GTG-banding in a case of AIDS-related Burkitt's lymphoma. *Haematologica* 2000; **85**:250-255.

14. Reddy KS, Parsons L, Mak L, Chan JA. An *hsr* on chromosome 7 was shown to be an insertion of four copies of the 11q23 MLL gene region in an HIV-related lymphoma. *Cancer Genet Cytogenet* 2001; **129**:107–111.
15. Zou H, McGarry TJ, Bernal T, Kirschner MW. Identification of a vertebrate sister-chromatid separation inhibitor involved in transformation and tumorigenesis. *Science* 1999; **285**:418–422.
16. Michel LS, Liberal V, Chatterjee A, Kirchwegger R, Pasche B, Gerald W, et al. MAD2 haplo-insufficiency causes premature anaphase and chromosome instability in mammalian cells. *Nature* 2001; **409**:355–359.
17. Babu JR, Jeganathan KB, Baker DJ, Wu X, Kang-Decker N, van Deursen JM. Rae1 is an essential mitotic checkpoint regulator that cooperates with Bub3 to prevent chromosome missegregation. *J Cell Biol* 2003; **160**:341–353.
18. Wittmann T, Hyman A, Desai A. The spindle: a dynamic assembly of microtubules and motors. *Nat Cell Biol* 2001; **3**:E28–E34.
19. Sumara I, Vorlaufer E, Gieffers C, Peters BH, Peters J-M. Characterization of vertebrate cohesin complexes and their regulation in prophase. *J Cell Biol* 2000; **151**:749–761.
20. Liu S-T, Hittle JC, Jablonski SA, Compbell MS, Yoda K, Yen TJ. Human CENP-I specifies localization of CENP-F, MAD1 and MAD2 to kinetochores and is essential for mitosis. *Nature Cell Biol* 2003; **5**:341–345.
21. Tang Z, Sun Y, Harley SE, Zou H, Yu H. Human Bub1 protects centromeric sister-chromatid cohesion through Shugosin during mitosis. *Proc Natl Acad Sci U S A* 2004; **101**:18012–18017.
22. Obuse C, Iwasaki O, Kiyomitsu T, Goshima G, Toyoda Y, Yanagida M. A conserved Mis 12 centromere complex is linked to heterochromatic HP1 and outer kinetochore protein Zwint-1. *Nat Cell Biol* 2004; **6**:1135–1141.
23. Fitzgerald PH, McEwan CM. Total aneuploidy and age-related sex chromosome aneuploidy in cultured lymphocytes of normal men and women. *Hum Genet* 1977; **39**:329–337.
24. Madan K, Lindhout D, Palan A. Premature centromere division (PCD): a dominantly inherited cytogenetic anomaly. *Hum Genet* 1987; **77**:193–196.
25. Bajnóczyk K, Gardó S. "Premature anaphase" in a couple with recurrent miscarriages. *Hum Genet* 1993; **92**:338–390.
26. German J. Roberts syndrome. I. Cytological evidence for a disturbance in chromatid pairing. *Clin Genet* 1979; **16**:441–447.
27. Petrinelli P, Antonelli A, Marcucci L, Dallapiccola B. Premature centromere splitting in a presumptive mild form of Roberts syndrome. *Hum Genet* 1984; **66**:96–99.
28. Kajii T, Kawai T, Takumi T, Misu H, Mabuchi O, Takahashi Y, et al. Mosaic variegated aneuploidy with multiple congenital abnormalities: homozygosity for total premature chromatid separation trait. *Am J Med Genet* 1998; **78**:245–249.
29. Kajii T, Ikeuchi T, Yang Z-Q, Nakamura Y, Tsuji Y, Yokomori K, et al. Cancer-prone syndrome of mosaic variegated aneuploidy and total premature chromatid separation: report of five infants. *Am J Med Genet* 2001; **104**:57–64.
30. Zhu D, Ma MS, Zhao RZ, Li MY. Centromere spreading and centromeric aberrations in ovarian tumors. *Cancer Genet Cytogenet* 1995; **80**:63–65.
31. Thompson PW, Davies SV, Whittaker JA. C-anaphase in a case of acute nonlymphocytic leukemia. *Cancer Genet Cytogenet* 1993; **71**:148–150.
32. Taguchi T, Shimura M, Osawa Y, Suzuki Y, Mizoguchi I, Niino K, et al. Nuclear trafficking of macromolecules by an oligopeptide derived from Vpr of human immunodeficiency virus type-1. *Biochem Biophys Res Commun* 2004; **320**:18–26.
33. Tokunaga K, Greenberg ML, Morse MA, Cumming RI, Lyerly HK, Cullen BR. Molecular basis for cell tropism of CXCR4-dependent human immunodeficiency virus type 1 isolates. *J Virol* 2001; **75**:6776–6785.